AEDC-TR-73-57

APPLICATION OF THE VORTEX-LATTICE METHOD TO REPRESENT A JET EXHAUSTING FROM A FLAT PLATE INTO A CROSSFLOWING STREAM

F. L. Heltsley and R. L. Parker, Jr.

ARO, Inc.

June 1973

ARNOLD ENGINEERING DEVELOPMENT CENTER
AIR FORCE SYSTEMS COMMAND
ARNOLD AIR FORCE STATION, TENNESSEE

NOTICES

When U. S. Government drawings specifications, or other data are used for any purpose other than a definitely related Government procurement operation, the Government thereby incurs no responsibility nor any obligation whatsoever, and the fact that the Government may have formulated, furnished, or in any way supplied the said drawings, specifications, or other data, is not to be regarded by implication or otherwise, or in any manner licensing the holder or any other person or corporation, or conveying any rights or permission to manufacture, use, or sell any patented invention that may in any way be related thereto.

Qualified users may obtain copies of this report from the Defense Documentation Center.

References to named commercial products in this report are not to be considered in any sense as an endorsement of the product by the United States Air Force or the Government.

APPLICATION OF THE VORTEX-LATTICE METHOD TO REPRESENT A JET EXHAUSTING FROM A FLAT PLATE INTO A CROSSFLOWING STREAM

F. L. Heltsley and R. L. Parker, Jr.
ARO, Inc.

FOREWORD

The work reported herein was conducted by the Arnold Engineering Development Center (AEDC) under sponsorship of the Air Force Flight Dynamics Laboratory (AFFDL), Air Force Systems Command (AFSC), under Program Element 64207F, Project 69BT.

The results presented were obtained by ARO, Inc. (a subsidiary of Sverdrup & Parcel and Associates, Inc.), contract operator of AEDC, AFSC, Arnold Air Force Station, Tennessee. The study was conducted from July 1, 1970, to June 30, 1972, under ARO Project No. BC5132. The manuscript was submitted for publication on October 25, 1972.

This technical report has been reviewed and is approved.

CARLOS TIRRES
Capt, USAF
Research and Development Division
Directorate of Technology

ROBERT O. DIETZ
Director of Technology

ABSTRACT

A study was conducted to develop a mathematical model of a jet exhausting from a flat plate into a crossflowing stream. The modeling was accomplished using the vortex-lattice method. Analytical streamlines and pressure distributions on the flat-plate surface as well as vector data in the field above the plate are compared with available experimental data. Recommendations are made for further improvement of vortex-lattice jet-modeling techniques.

CONTENTS

APPENDIXES

I. ILLUSTRATIONS

Figure

NOMENCLATURE

C_p	Pressure coefficient, $(p_- p_\infty)/q$
D	Jet exit diameter, ft
P	Pressure, lb/ft^2
q	Dynamic pressure, lb/ft^2
R	Jet exit radius, ft
V	Velocity, ft/sec
Ve	Effective velocity ratio, $\sqrt{\frac{\rho_\infty V_\infty^2}{\rho_j V_j^2}}$
X, Y, Z	Coordinates related to free-stream velocity
δ	Deflection of jet-exit centerline, positive with increasing angle away from free-stream, deg
ρ	Density, $slugs/ft^3$

SUBSCRIPTS

j	Jet exit
∞	Free stream

SECTION I
INTRODUCTION

Much work has been done to define the characteristics of jets exhausting into a crossflowing stream. Numerous experimental programs have been performed to gain insight into the behavior of these jets and their mutual interaction with the surrounding fluid. Schemes for analytically duplicating the complex flow fields associated with jets have been developed, with varying degrees of success, by a number of individuals.

This report presents the results of an attempt to apply a previously developed theory for representing jet plumes to a configuration in which the jet exhausts from a flat plate. The technique presented allows computation of pressures and streamlines on the flat plate. Velocity vectors, streamlines, and pressures can be calculated throughout the flow field surrounding the jet plume. The method does not require a great deal of computer time, even though it is capable of handling complex configurations of multiple jets and solid surfaces.

SECTION II
PROPERTIES OF THE JET

The vortex-lattice model described in this paper is an attempt to simulate the physical phenomena observed in jets exhausting into crossflows. Consideration is given to representing the effect of the jet upon the surrounding flow field and the flat-plate surface. Simulation of the internal flow is ignored. Therefore, it is necessary to have a basic understanding of the properties of such jets and the associated aerodynamic characteristics.

The jet exiting a surface enters the stream normally (i. e., without the skew angle exhibited in the free-jet case). As the jet exhausts from the surface, it is bent in the direction of the crossflowing stream because of two primary mechanisms. The major cause is the momentum transfer due to turbulent shear forces acting on the lateral regions of the jet. This results in general sweeping downstream as fluid from the crossflow is entrained into the jet. A smaller influence on the jet bending results from the pressure differential across the jet. Several investigations have been conducted to define the jet deflection, and

numerous empirical relationships have been derived for the axial centerline trajectory. All agree that the jet path trajectory is mainly a function of the velocity ratio. The expression used in this development was provided by Margason (Ref. 1), as follows:

$$\frac{X}{D} = - \frac{V_e^2}{4 \sin^2 \delta_j} \left(\frac{Z}{D}\right)^3 - \frac{Z}{D} \cot \delta_j$$

Since the sides of the jet are deflected downstream more rapidly than the core, the cross section takes on the classical crescent shape. This eventually results in a rollup of the jet and formation of two contrarotating vortices which endure relatively far downstream and then finally submit to viscous effects.

As the jet penetrates the crossflowing stream, its cross section increases in size because of both expansion and the addition of free-stream fluid. The two mechanisms responsible for this addition of fluid have been dubbed turbulent and nonturbulent entrainment. Turbulent entrainment takes place in the regions of turbulent mixing. This is the same means by which jets exhausting into quiescent air entrain and is caused by mean velocity differences within the flow. Nonturbulent entrainment is primarily a result of the contrarotating vortex pair. Free-stream fluid is swept around the sides of the jet and is captured by the jet rollup process. Previous studies indicate that entrainment caused by the latter pressure-induced phenomena may be an order of magnitude greater than that caused by the viscous mechanism.

A jet exhausting into a crossflow displays a low-pressure wake region on the downstream side. It has been shown that the jet exhibits a blockage similar to a cylinder with suction. As free-stream fluid approaches the jet, it is first influenced by the blockage effect. It is deflected outward and upward by the contrarotating vortices and is either captured by one of the entrainment mechanisms or swept into the aft wake region. A number of plots of the q-vector data given by D. K. Mosher (Ref. 2) are shown in Fig. 1, Appendix I. Note that without a knowledge of the total pressure values it is impossible to distinguish the jet from the free stream, since sharp discontinuities in flow direction occur only near the jet exit.

A major portion of jet investigations have dealt with the pressure field induced on the surface from which the jet exhausts. In V/STOL

applications, a primary concern is the lift loss caused by the jet. Practical application of an analytical model requires accurate simulation of this phenomenon.

Pressures on the surface are known to be affected by a combination of blockage and entrainment mechanisms. Mosher's study indicates that both mechanisms exert influence at low velocity ratios; however, entrainment effects dominate as the velocity ratio increases. Blockage affects the areas immediately to the front and rear of the jet, whereas entrainment effects encompass all the remaining areas. Plate pressure contours from Ref. 2 are shown in Fig. 2 for a variety of velocity ratios. As the flow approaches the jet, it is decelerated because of the blockage, and a small positive pressure area is formed. The flow is then diverted around the jet and is accelerated, resulting in a negative pressure region on the sides of the jet. The contrarotating vortices have a major effect on the plate flow as they entrain fluid. They cause an insweep of flow to the sides of the jet, resulting in a sink-like pattern which causes negative pressure regions far from the jet sides.

When the velocity ratio is increased, the entrainment mechanism becomes stronger. The positive pressure region forward of the jet is diminished in both size and magnitude, and the negative areas to the sides and rear expand and become more negative. Finally, at some velocity ratio, the positive region will disappear. It should be noted that several authors have carried out similar investigations and have arrived at the same general conclusion (Refs. 2, 5, 6, and 7). Data from these experiments are available in the literature.

Additional information concerning the flow over the plate surface can be obtained through the use of oil-film traces. The result of an oil study conducted by Mosher appears in Fig. 3 along with the authors' interpretation of the plate surface streamlines. As the figure shows, the flow into the region aft of the jet exit is not continuous. A pair of stagnation lines is shown extending downstream from the back of the exit. It is evident that the lines result from a pair of contrarotating eddies which lie very near the plate surface. The disturbances from these eddies are not believed to extend far up into the wake region, although no quantitative flow-field data could be found in the literature defining the volume in the vicinity of the plate. However, the vector information recorded in Ref. 2 shows that no disturbance occurs beyond two diameters above the surface. Since the analytical model described in this document provides no means for representing these eddies, the stagnation lines are not expected to appear in the computed flow pattern on the plate.

SECTION III
JET MODEL CONSTRUCTION

Reference 3 presents the development of a general jet efflux representation by the vortex-lattice method. This jet model is composed of an inlet simulation and exhaust blockage represented by lifting vortex panels. Given the velocity ratio, a computer program automatically computes the trajectory, inlet skew angle, and tube geometry. This model was used to simulate a free propeller submerged in a crossflow.

Preparation of an analytical model for a jet exhausting from a flat plate required four basic changes to the previously developed propeller jet representation. The vena contracta associated with the propeller was removed, leaving a vortex-lattice tube of uniform cross section. The tube axis was forced to intersect the jet-face plane at an angle of 90 deg, rather than at the skew angle computed from the velocity ratio (i. e., V_j/V_∞). In the initial configuration, a large, flat vortex grid was attached to the jet face to represent an infinite flat plate. The nonuniform inlet velocity distribution was replaced by a uniform one.

The modified configuration representing a jet exhausting from a plate at twice the free-stream velocity is shown in Fig. 4. Several problems were apparent with this initial configuration. Addition of the flat-plate grid severely increased the turn-around time for obtaining digital computer solutions. The expanding nature of the plate grid spacing resulted in poor simulation of a flat plate, since leaks occurred in some areas. With the vortex-lattice program, pressures on a surface can be computed only at control point locations. The flat-plate grid limited the pressure distribution computations to these points. One possibility for improvement was to replace the expanding octagonal grid with a much tighter rectangular one with uniform spacing. However, this solution would greatly increase the computer time required. A better solution involved using the symmetry-plane capability of the computer program. Since no flow is allowed to pass through the plane of symmetry, it provides an ideal infinite plate representation.

A verification study was conducted to prove the validity of the symmetry application to this particular problem. Figure 5 is a schematic of the three configurations which were examined. The configurations were intended to analytically duplicate the experiment conducted by Mosher in the Georgia Institute of Technology 9-ft-diam wind tunnel (Ref. 2). As Fig. 5 indicates, the region of interest included the lower

surface of the plate and the volume surrounding the jet. Although an inlet was simulated on the side of the plate away from the jet, its effect upon the cross-hatched region was deemed negligible, assuming the plate to be infinite. The model shown in Fig. 5b was investigated to define the inlet effect upon the flow beneath the plate and to determine the feasibility of shutting off the flow through the vortex tube. As was expected, computations indicated that pressures on the underside of the plate were unchanged except near the outside edges. The absence of flow exhausting from the vortex tube jet efflux simulation resulted in slight changes in the flow field near the tube exit; however, no variation was observed within the region of interest. The final configuration, illustrated in Fig. 5c, produced results very similar to those of the model shown in Figs. 5a and b. Use of the symmetry plane to replace the vortex grid removed the plate edge effect entirely. In addition, removal of the grid reduced to zero the disturbances generated by the individual vortex elements. Since no other changes could be detected in the region of interest, the symmetry plane model was chosen as the configuration to be used in the subsequent investigation.

With respect to the relative orientation of the individual vortex panels, the model illustrated in Fig. 5c is identical to the free propeller model presented in Ref. 3. However, use of the mirror image plate representation requires omission of the inlet grid and the associated tube exit ring along with a rotation of the entire vortex network. This is necessary because the computer program is limited to providing for symmetry about the Y = 0 plane. It should be noted that only the input portion of the vortex network is shown in the figure. The reflected portion of the mathematical representation is handled internally by the program.

SECTION IV
PARAMETRIC STUDY

Upon completion of the vortex-lattice model preparation, an attempt was made to evaluate the new configuration by comparing analytically generated data with experimental results. In an effort to more closely simulate the experimental phenomena and test the sensitivity of the model under various conditions, changes were made in a number of parameters. The parameters selected included width and shape of the trailing vortex sheet and entrainment rate through the vortex tube wall. Information gained in such an investigation would be of value in

the extension of the jet representation to other velocity ratios. The model used as a basis for this portion of the study is shown in Fig. 6. A jet-to-free-stream velocity ratio of eight was used to define the tube trajectory. The boundary conditions controlling entrainment through the tube walls were set at zero. The effective jet expansion rate and width of the trailing sheet remained the same as those used originally on the propeller configuration. In order to accomodate the change in jet trajectory, however, the vortex spacing along the tube was modified. The distance from the jet exit to the first tube ring was increased to two and one-half times the nondimensional value used in the propeller configuration. The parameter which controls the spacing increment of the remaining tube ring stations was increased by a factor of five. These changes were made to lengthen the lattice tube and remove the tube exit from the region of interest. In addition to these and other geometrical changes in the model, computations were made for a variety of entrainment rates.

Five-digit numbers were used to identify the various models investigated during this study. The significance of each digit is given in Table I, Appendix II, along with the implication of various digit values. The number "1. 0000" was chosen to represent the model described above. Figure 7 illustrates the configurations investigated along with the corresponding model identification numbers.

Three types of analytical data were correlated with experimental information. These were pressure distributions and streamlines on the flat plate surface, and velocity vectors at selected points in the flow field about the jet. The results of the investigation are described in the following paragraphs.

Analytical solutions for the initial configuration, Model 1. 0000, produced flow characteristics considerably different from those observed by Mosher. Although a contrarotating vortex pair was present in the analytical flow field, the sense was reversed from that of the vortices within a real jet. Addition of an entrainment velocity to the tube surface boundary conditions resulted in significant changes in the associated flow field. As is shown by the vectors in Fig. 8, the sense of the vortex pair was corrected. The circulation was increased to the extent that fluid was forced through the tube lattice. This is illustrated by the streamlines on the plate surface shown in Fig. 9 for three entrainment values. Note that the leakage produces streamlines similar to those generated by a two-dimensional doublet-sink combination except in the region downstream of the jet tube. The high velocities

associated with the strong recirculation are reflected in the pressure distribution on the plate surface, as can be seen in Fig. 10.

On the basis of this information, it appeared that any improvement in the analytical flow characteristics would require reduction of the recirculation being generated by the vortex pair. Previous experience had shown that this recirculation could be reduced by reducing the trailing vortex sheet width. The shape of the sheet attached to the x. x0xx series models was identical to that used on the propeller jet configuration described in Ref. 3. Although the propeller jet had been developed for a velocity ratio of 2. 14, no attempt had been made to modify the sheet contour for the plate-jet combination, since no suitable expirical data could be found for a velocity ratio of 8. 0. In the absence of such information, an intuitive guess was made as to the proper sheet contour. It is known that rollup of the jet occurs farther along the trajectory for increasing velocity ratios. To more closely represent the rollup phenomenon, it was decided to elongate the vortex sheet shape.

As shown in Fig. 11, the high recirculation was reduced. In fact, the streamlines are seen to closely resemble those about a two-dimensional potential cylinder. The plot of the plate pressure distribution shown in Fig. 12 was also somewhat promising. The pressures in the regions fore and aft of the jet were much reduced, although the aft zero pressure line was moved outward, further increasing the size of the positive pressure region. The extreme low pressures on either side of the jet were overrelieved and ended up somewhat higher than the experimental values.

Encouraged by the reduction in the recirculation characteristic and the favorable plate pressure distribution, the authors decided to resume the increase in entrainment rate through the jet-tube surface. Plate surface streamlines generated for increased values of entrainment are shown in Fig. 13. The trend suggests that an even higher value is in order if the experimental surface pattern is to be matched. Examination of the surface pressure distribution, however, indicates that the increase in entrainment value from Model 1. 2100 and Model 1. 4100 was already too large for this particular configuration. Figure 14 shows that the pressures on either side of the tube are lower than the experimental data. It is interesting to note that the increase in entrainment caused a universal decrease in pressure over the plate and that both positive pressure regions were drastically reduced in size. Figure 15 shows the effect of further decreasing the entrainment. It is evident that excessive circulation is produced in the jet cross section. This

results in velocities considerably higher than those measured near the real jet.

Model 1.4110 was generated in an attempt to improve the plate streamlines without degrading either the flow field below the plate or the plate pressure distribution. As Figs. 16 and 17 show, the attempt was unsuccessful. The flow field exhibited the same severe recirculation and leakage through the jet-tube surface which had previously appeared in Model 1.3000.

As a final attempt to improve the analytical jet representation by reduction of the leakage through the jet-tube surface, the x.x101 series of models was generated. The new configuration was identical to the x.x100 model series except for a closer spacing of the vortex grid along the jet tube. Both the initial space width and the spacing increment were reduced by 50 percent. Since no additional vortex filaments were added to the model, however, the modification resulted in a shorter jet tube.

The changes in configuration resulted in a reverse in sense of the circulation within the jet cross section. The effect can be seen both in the plate streamlines and in the flow field around the jet, as shown in Figs. 18 and 19, respectively. Computations indicated that the reversal occurred for a wide range of entrainment rates. Although it has not been demonstrated, the authors feel that the addition of vortices to the model was not directly responsible for the problem. Modification for tighter vortex spacing significantly shortened the tube. Since the computer program automatically trails the vortices to infinity after the last vortex ring, a severe change occurs in the effective jet trajectory. This is shown schematically in Fig. 20. In this configuration the tube exit and the associated trailing vorticity fall very near the region of interest. The situation is further complicated by the fact that the discontinuity occurs near the point of maximum jet bending rate.

SECTION V
CONCLUSIONS

During the course of the investigation a number of conclusions were drawn prior to the choice of the basic vortex configuration, Model 1.0000. Many have been discussed previously and are reiterated here for the convenience of the reader. Others are included for the first time. Conclusions are as follows:

1. Preliminary investigation indicated that the plane-of-symmetry technique could be successfully applied to the jet-plate combination. This was possible for two reasons: first, the flow characteristics within the jet tube were of no interest, and second, an infinite flat plate was being simulated. Use of this technique simplified the analytical modeling, permitted a reduction in computer time required, and provided a means of eliminating the complications involved in representing the plate with a vortex grid. It should be pointed out that general analytical modeling situations involve inlets, curved surfaces, and multiple jets. Consequently, the user is deprived of the luxury of using the symmetry plane to represent the surface from which the jet emerges. In many cases, however, symmetry does exist in the flow field, and time can be saved through use of the plane-of-symmetry technique.

2. In situations where inlets are present, caution should be exercised in the positioning of the vortex tube exit. Flow expanding from the tube exit can severely interfere with the surrounding flow field, especially when high jet velocities are to be simulated. Therefore, the tube should be extended sufficiently far downstream to render the effects of the expanding fluid negligible.

3. Initial computations for Model 1.0000 revealed that the trailing sheet circulation was opposite in direction from that existing within a real jet. It was shown that the addition of entrainment through the tube surfaces could correct the situation. The requirement for additional entrainment, however, resulted in a severe recirculation and in leakage through the tube walls. Similar conditions could be generated by widening the trailing sheet, as shown by Model 1.4110.

4. With respect to the flat-plate pressure distribution, it was found that high entrainment values could result in excessively low pressures on either side of the jet. The study indicated that a nearly identical pressure distribution was produced each time the recirculation occurred.

5. The attempt to eliminate the recirculation by tightening the jet-tube lattice spacing proved to be unsuccessful. However, the reappearance of the reverse circulation was thought to be caused by the shortening of the tube rather than by the closer spacing of the vortices.

6. Of the various configurations investigated, Model 1.4100 provided the best correlation with experimental data. Comparisons of the analytical and empirical results are presented in Figs. 21, 22, and 23. Vectors throughout the flow field surrounding the jet efflux were in excellent agreement. However, based upon the trends established by variation of entrainment, the optimum plate pressure distribution would occur at a slightly lower value than that used in Model 1.4100. With respect to streamlines on the plate surface, it appears that a higher entrainment value would have improved the data. This is more obvious if the streamlines interpreted from the oil-trace data shown in Fig. 5 are modified to remove the effect of the previously mentioned contrarotating eddies near the plate surface. The modified streamlines would represent the best possible results obtainable using an analytical model which did not include a provision for simulating the eddies. If the disturbances did not, in fact, extend far from the plate surface, the streamlines might closely resemble the flow field immediately past the eddies. Figure 24 is the authors' depiction of the proposed streamlines.

7. The discrepancies apparent in the model 1.4100 data suggest that a configuration modification is in order. It is the opinion of the authors that an attempt should be made to simulate both the wake region aft of the jet plume and the pair of eddies near the plate. However, no suitable technique is envisioned for a potential flow model such as the one discussed in this document.

SECTION VI
RECOMMENDATIONS

Model 1.4100 is capable of providing a quality of data which is far superior to that generated by most other analytical jet representations. However, it is not adequate for applications which require precise reproduction of the near flow field. The following comments are included in order to provide a starting point for further development of the plane-of-symmetry technique.

The classical method of improving any model generated using finite element theory involves increasing the number of elements. A point of diminishing returns is reached, however, when the improvement realized becomes smaller than the errors associated with the mismatch between the body being represented and the potential model. This is not to mention the drastic increases in computer time associated with the addition of vortex filaments. It is futile to exchange an octagonal vortex tube for one with twenty sides when the latter is capable of no more precise simulation of the real flow characteristics (i.e., viscous effects, wake, etc.) than is the former. The user might find it advantageous, however, to choose the octagonal tube over one of square cross section after examining the respective distances of singularity error propagation into the far flow field. It is the opinion of the authors that the octagonal tube used in this investigation is adequate for representating a real jet if the region of interest does not include the volume within one-half the diameter of the tube surface. Tighter spacing along the jet axis should provide better simulation if additional vortices are added to maintain the original tube length. The authors feel that the optimum model would be a twelve-sided tube with the vortices spaced evenly along the jet axis in such a manner that each individual vortex panel is nearly square.

After the original modeling was carried out, several improvements were added to the AEDC vortex-lattice computer program. Since the modified revision of the program does not limit "wing part" size, the analytical model could be greatly simplified by substituting one pair of "wing parts" for the two pairs currently used to make up the upstream half of the jet tube. Such a modification, however, would require a change in the method for distributing the "extra points" which define the trailing vortex sheet. A detailed description of the method is included as Ref. 3.

The trends established during the course of this investigation suggest that an even more narrow vortex sheet than that attached to Model 1.4100 might provide more realistic flow-field data. Such a modification would probably necessitate an increase in entrainment value, since the strength of the trailing sheet vorticity would more than likely be reduced. It would also be of interest to define vortex sheet shapes using the experimental data presented in both Refs. 2 and 4 and to compare them with the contour associated with Model 1.4100. In addition, it might be profitable to examine the flow about a configuration with the sheet collapsed against the side of the vortex tube. The authors have investigated such a model for the zero-entrainment case, and it is described in Ref. 3. The resulting flow field was found to be identical to that produced by an inlet-potential cylinder combination, showing poor correlation with experimental jet data.

Since the trend for a flat-plate jet model with entrainment seems to be toward the more narrow trailing sheet, i.e., closer to the plain cylinder case, there is a possibility that the real flow fields may be governed by different phenomena. It should be emphasized that in order to maintain similar flow conditions an increase in entrainment was required when the width of the trailing sheet was reduced. A more likely conclusion is that the two potential-flow mechanisms involved, namely tube surface entrainment and the trailing vortex pair, are responsible for the flow-field similarity. The addition of entrainment to the propeller model described in Ref. 3 might be a means of providing an insight into the situation.

Another avenue which has been virtually unexplored by the authors involves the application of an entrainment distribution around the jet tube, both around the periphery and along the axis. Although no suitable empirical data seem to be available, it may be possible to determine such distributions by computer experimentation. Various distributions can be chosen and the resulting flow fields compared to those provided by experiment.

Investigation of this approach should be extended to include other jet-to-free stream velocity ratios in an attempt to define the effects of that variable upon the analytical configuration. Such an effort, however, would require more empirical data than is presently available.

One additional recommendation is offered since it is somewhat related to the technique described in this report. The results previously presented indicate that a potential model with entrainment can produce

flow fields similar to those generated by a configuration with trailing vorticity. Jet cross-sectional shapes are obtainable from a number of existing experimental sources (e.g., Refs. 2 and 8). In addition, three-dimensional analytical schemes such as the one presented by Hackett and Miller in Ref. 5 are available. Based on the present study, a vortex-lattice tube with its shape derived from one of the above-mentioned sources and with a suitable entrainment distribution over the surface could provide improved analytical simulation of a real jet plume.

REFERENCES

1. Margason, Richard J. "The Path of a Jet Directed at Large Angles to a Subsonic Free Stream." NASA TND-4919, November 1968.
2. Mosher, David K. "An Experimental Investigation of a Turbulent Jet in a Cross Flow." GITAER 70-7, December 1970.
3. Parker, R. L., Jr. and Heltsley, F. L. "Simulation of a High Disc Loading Free Propeller in a Cross Flow by the Vortex-Lattice Method." AEDC-TR-72-139 (AD751463), November 1972.
4. Hackett, J. E. and Miller, H. R. "The Aerodynamics of the Lifting Jet in a Cross Flowing Stream." Paper in Analysis of a Jet in a Subsonic Crosswind. NASA SP-218, September 1969.
5. Bradbury, L. J. S. and Wood, M. N. "The Static Pressure Distribution Around a Circular Jet Exhausting Normally from a Plane Wall into an Airstream." RAE Tech Note AERO 2978, August 1964.
6. Vogler, Raymond D. "Surface Pressure Distributions Induced on a Flat Plate by a Cold Air Jet Issuing Perpendicularly from the Plate and Normal to a Low-Speed Free-Stream Flow." NASA TN D-1629, March 1963.
7. Gelb, G. H. and Martin, W. A. "An Experimental Investigation of the Flow Field About a Subsonic Jet Exhausting Into a Quiescent and a Low-Velocity Airstream." Can. Aeronaut. Space J., Vol. 12, No. 8 (Oct. 1966), pp. 333-342.
8. Kamotani, Y. and Greber, I. "Experiments on a Turbulent Jet in a Cross Flow." NASA CR-72893, June 1971.

APPENDIXES

I. ILLUSTRATIONS
II. TABLE

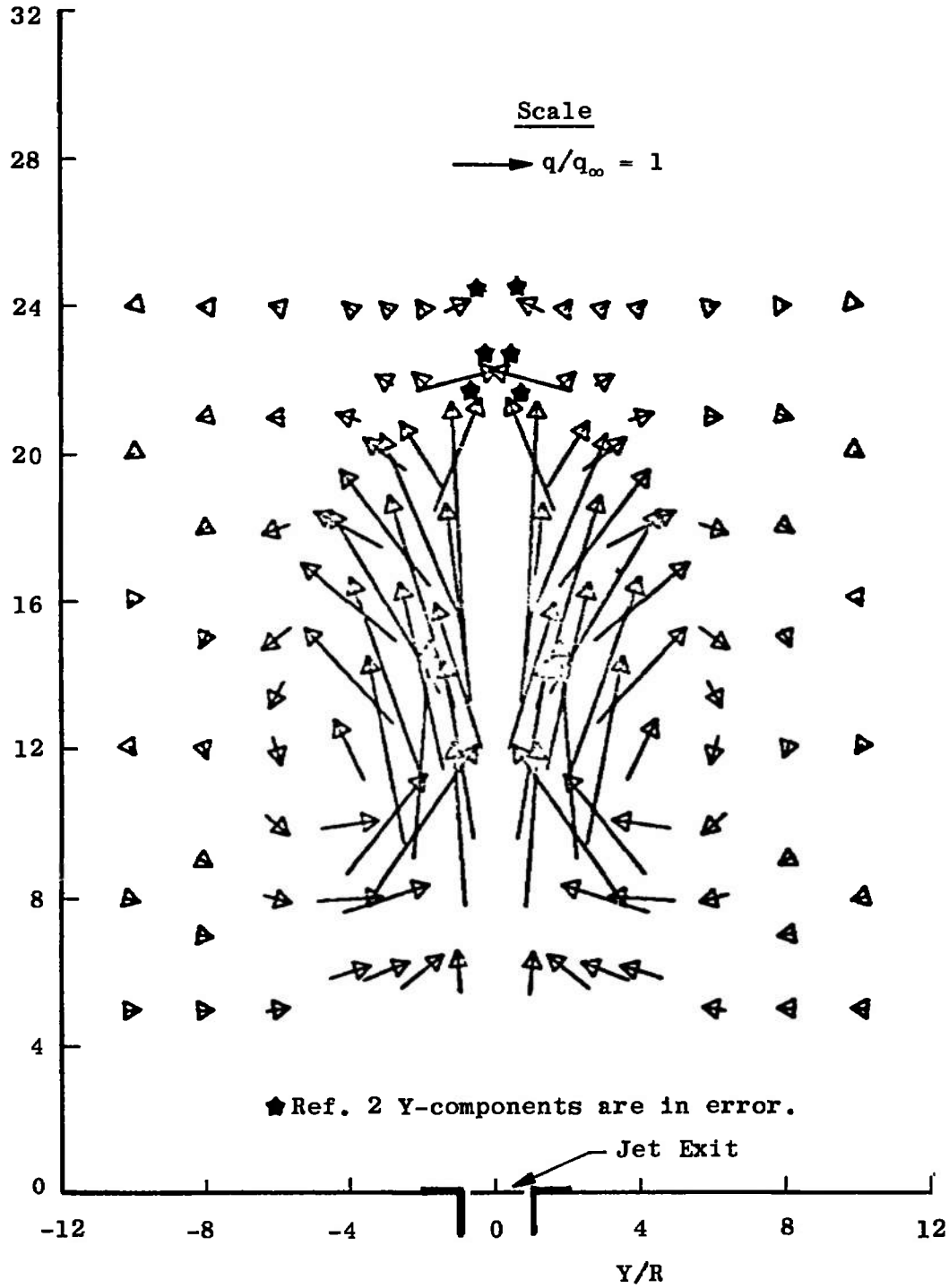

a. X/R = 6.000

Fig. 1 Jet in Crossflow q-Vector Projections, V_j/V_∞ = 8 (Ref. 2)

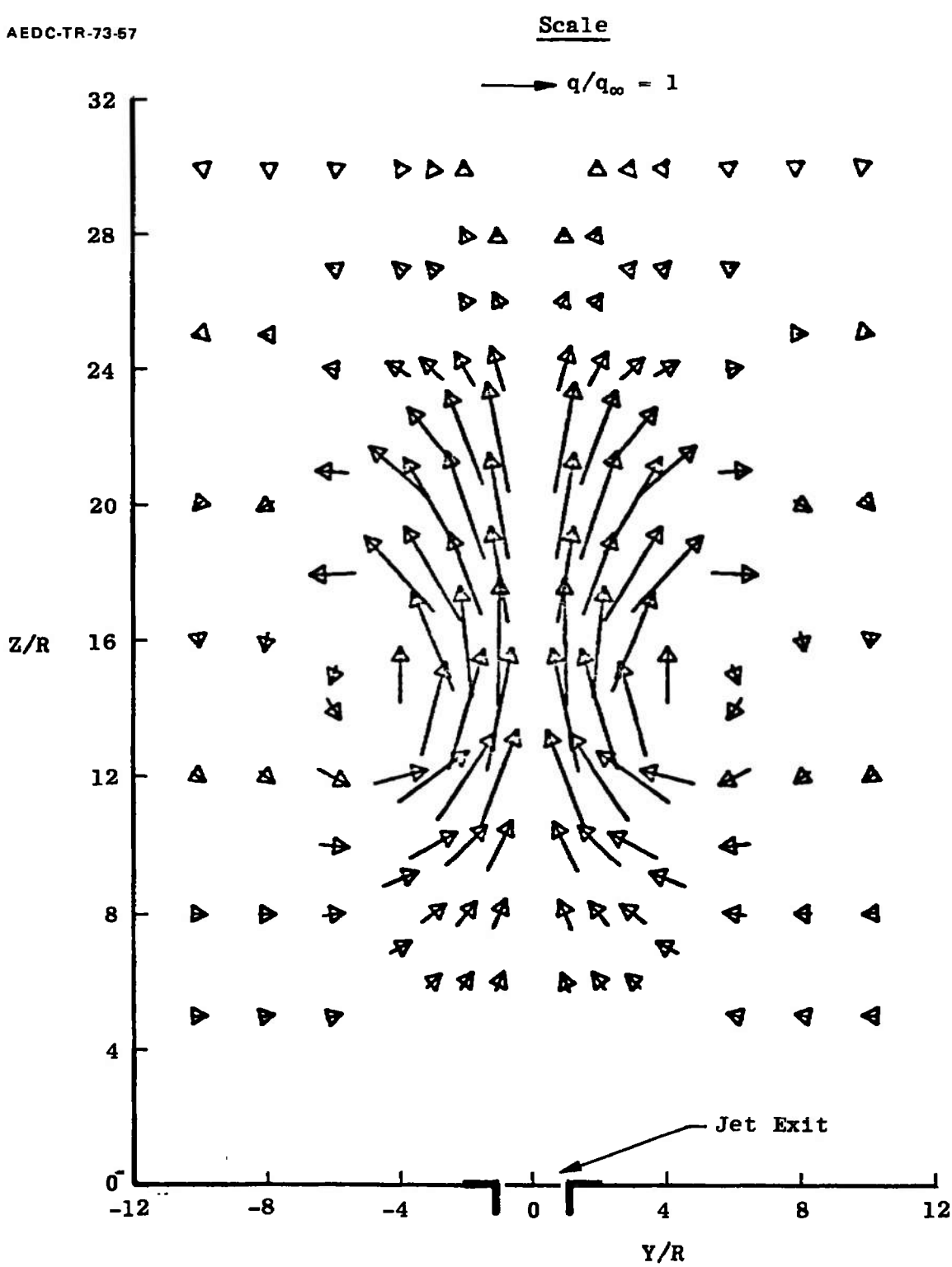

b. X/R = 10.000
Fig. 1 Continued

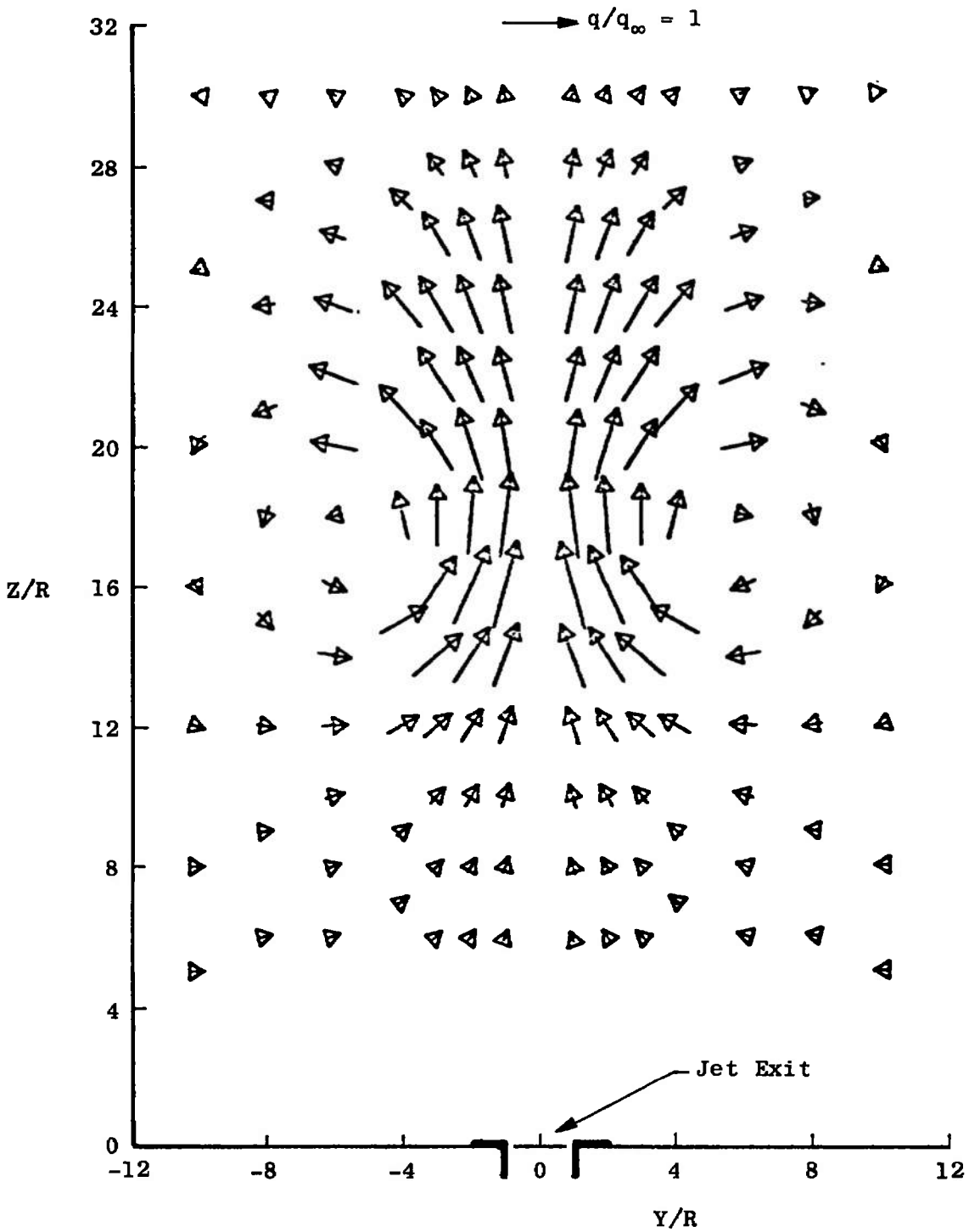

c. X/R = 16.000
Fig. 1 Continued

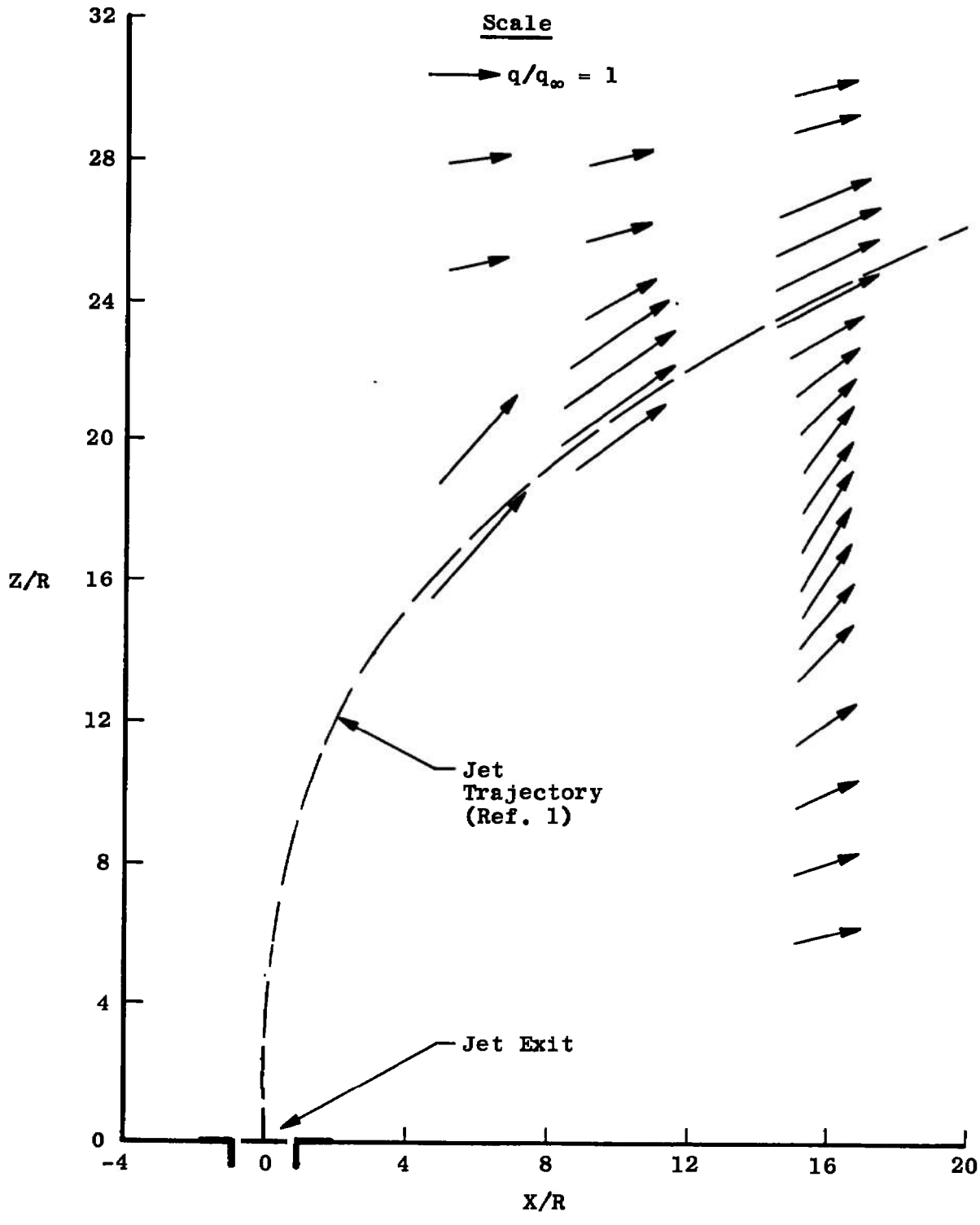

d. Y/R = 0

Fig. 1 Continued

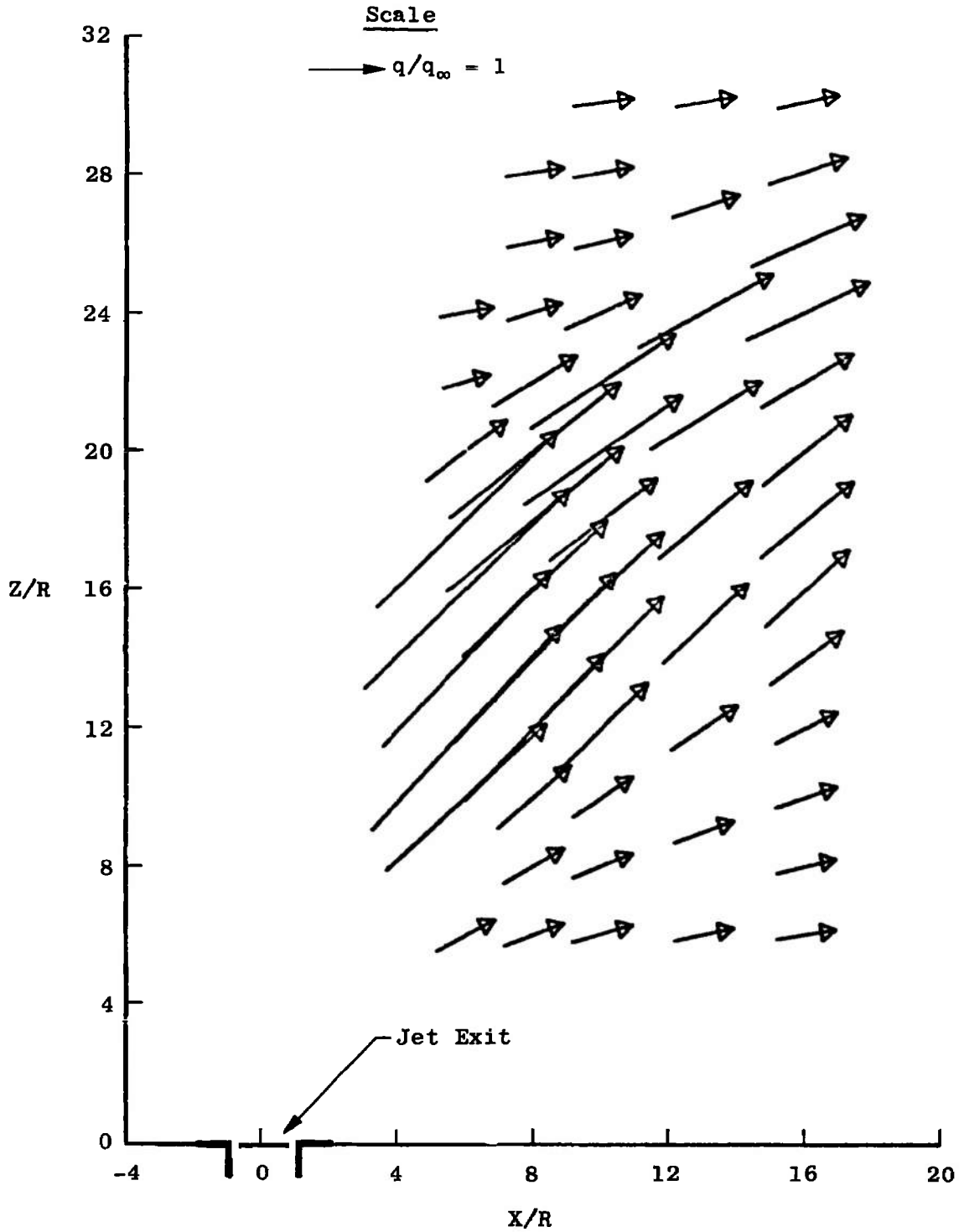

e. Y/R = 2.000
Fig. 1 Continued

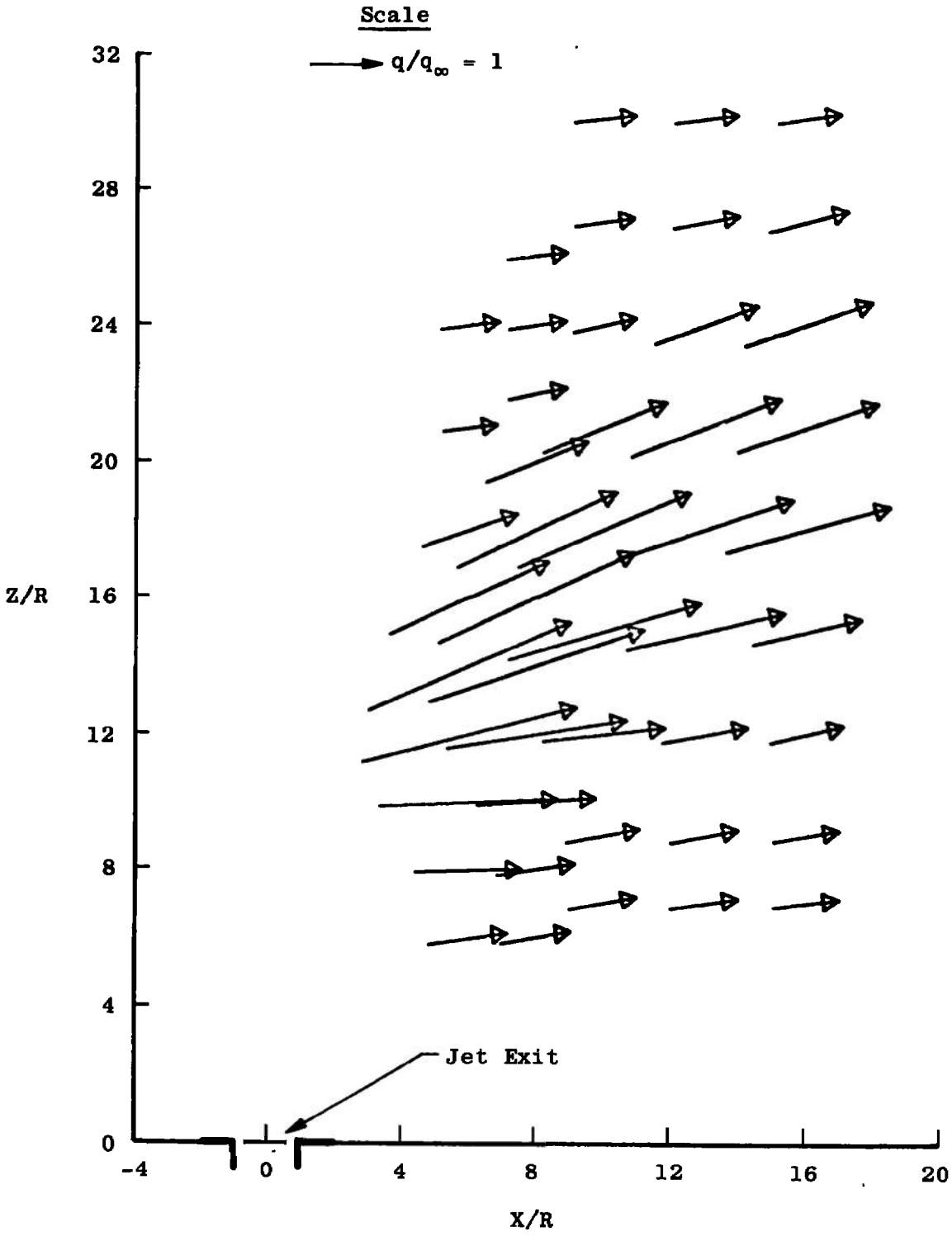

f. Y/R = 4.000
Fig. 1 Continued

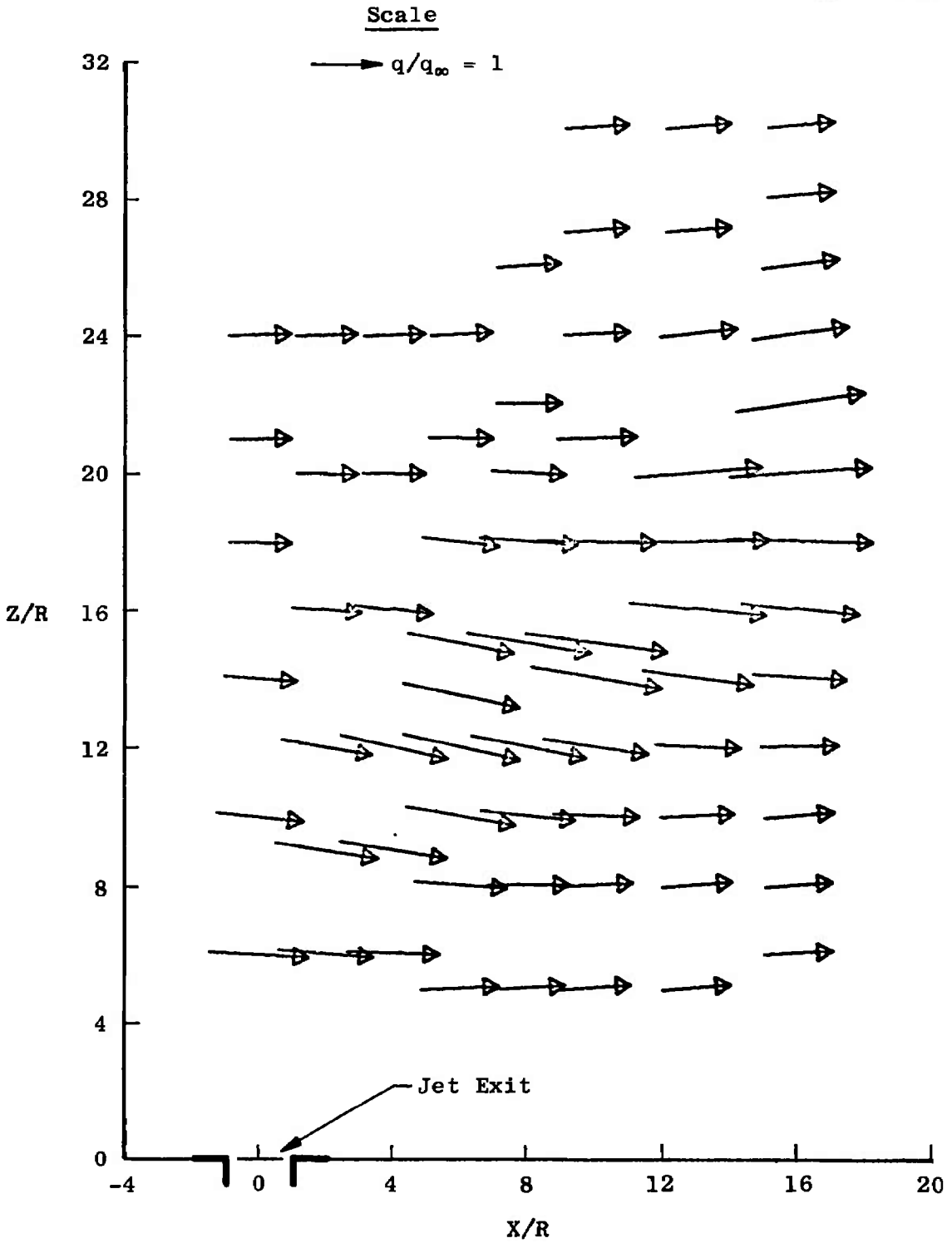

g. Y/R = 6.000
Fig. 1 Continued

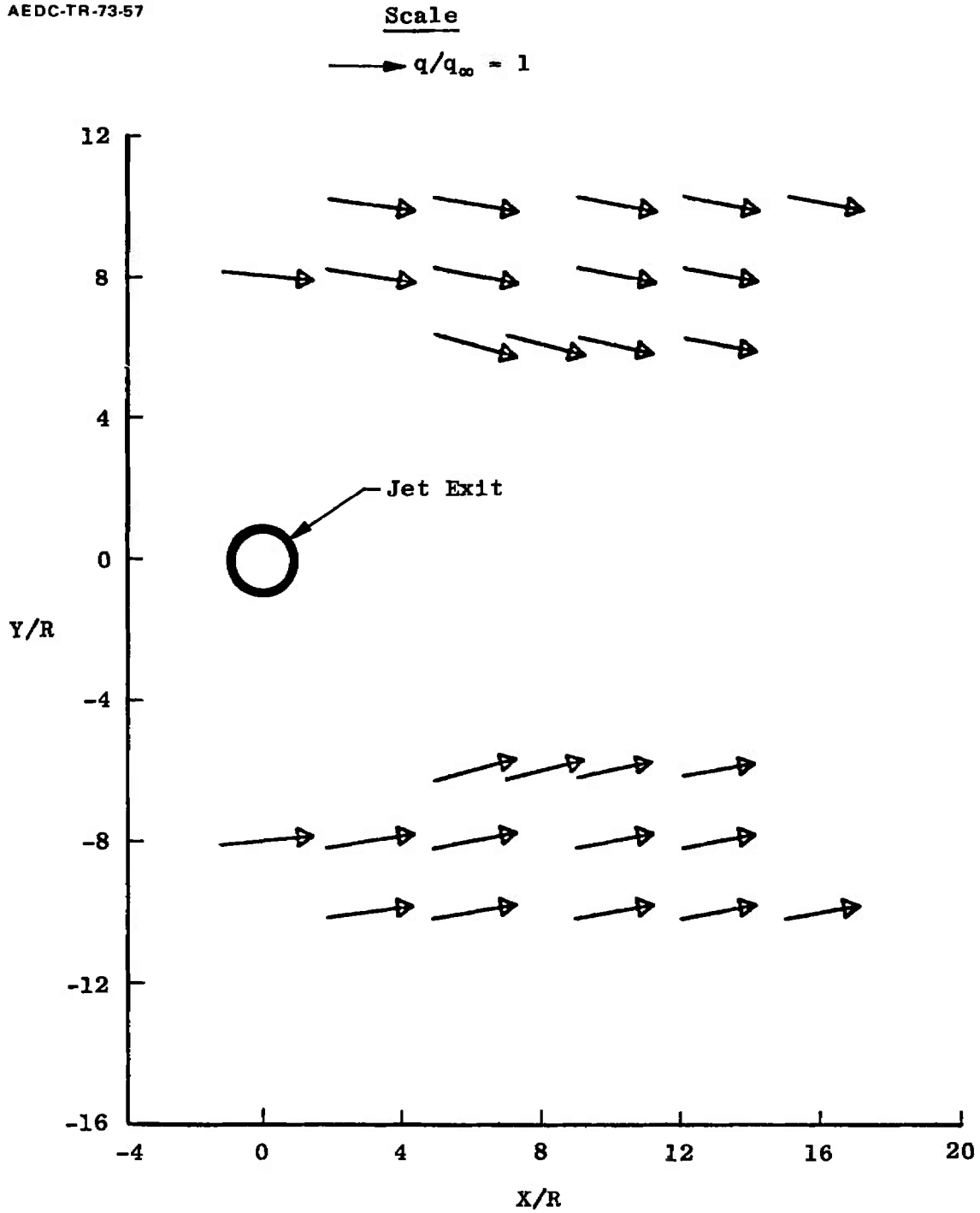

h. Z/R = 5.000
Fig. 1 Continued

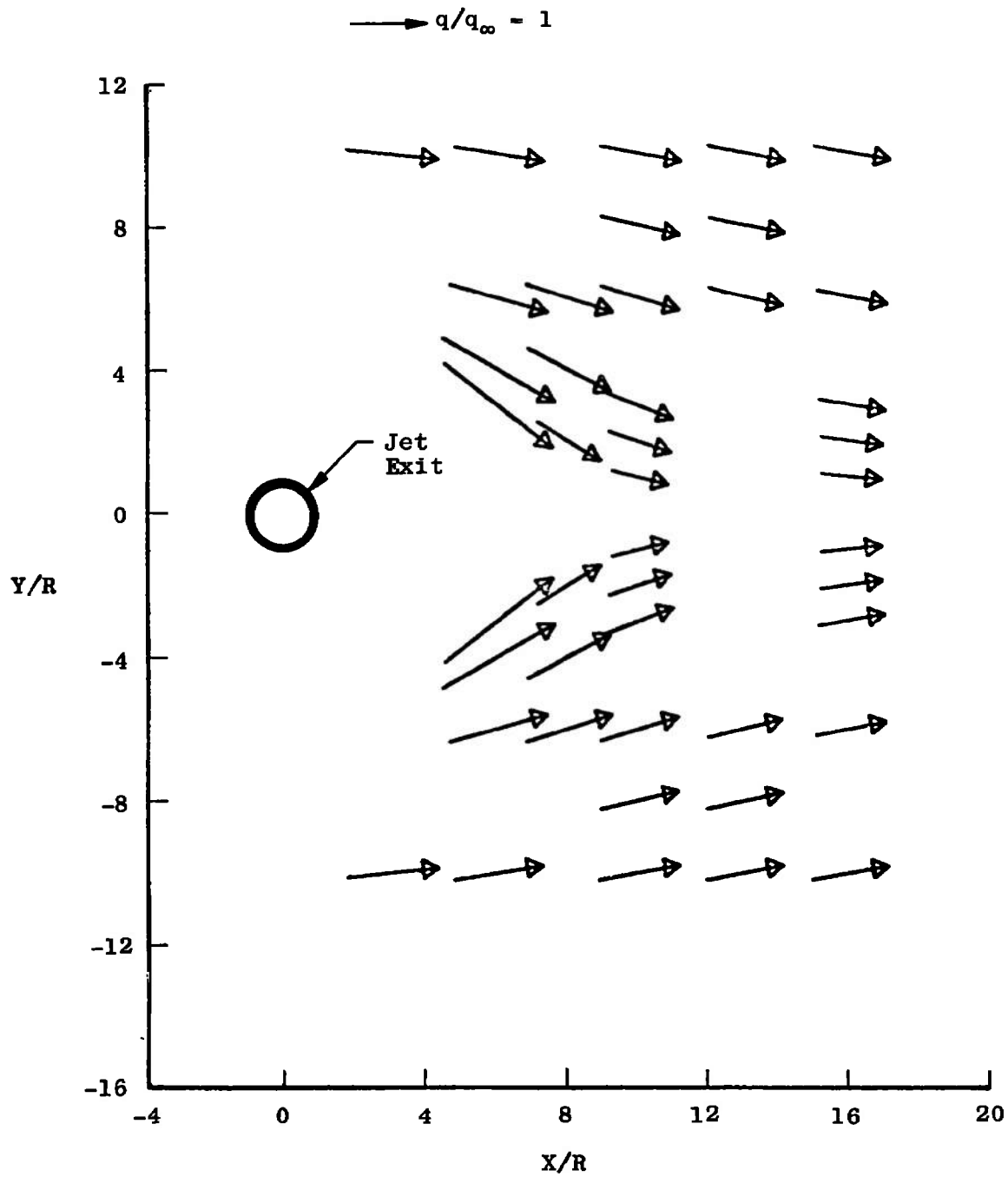

i. Z/R = 8.000
Fig. 1 Continued

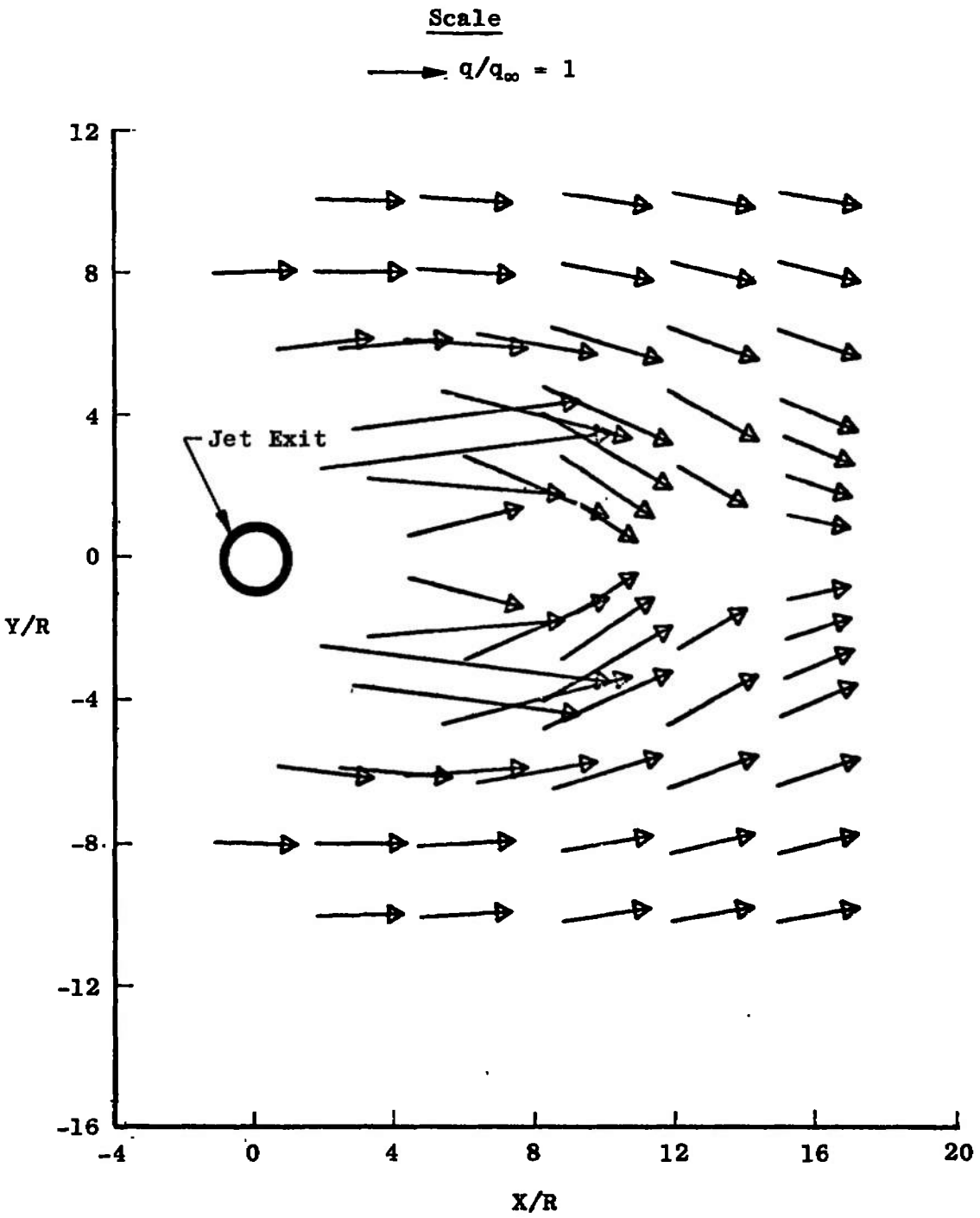

j. Z/R = 12.000
Fig. 1 Continued

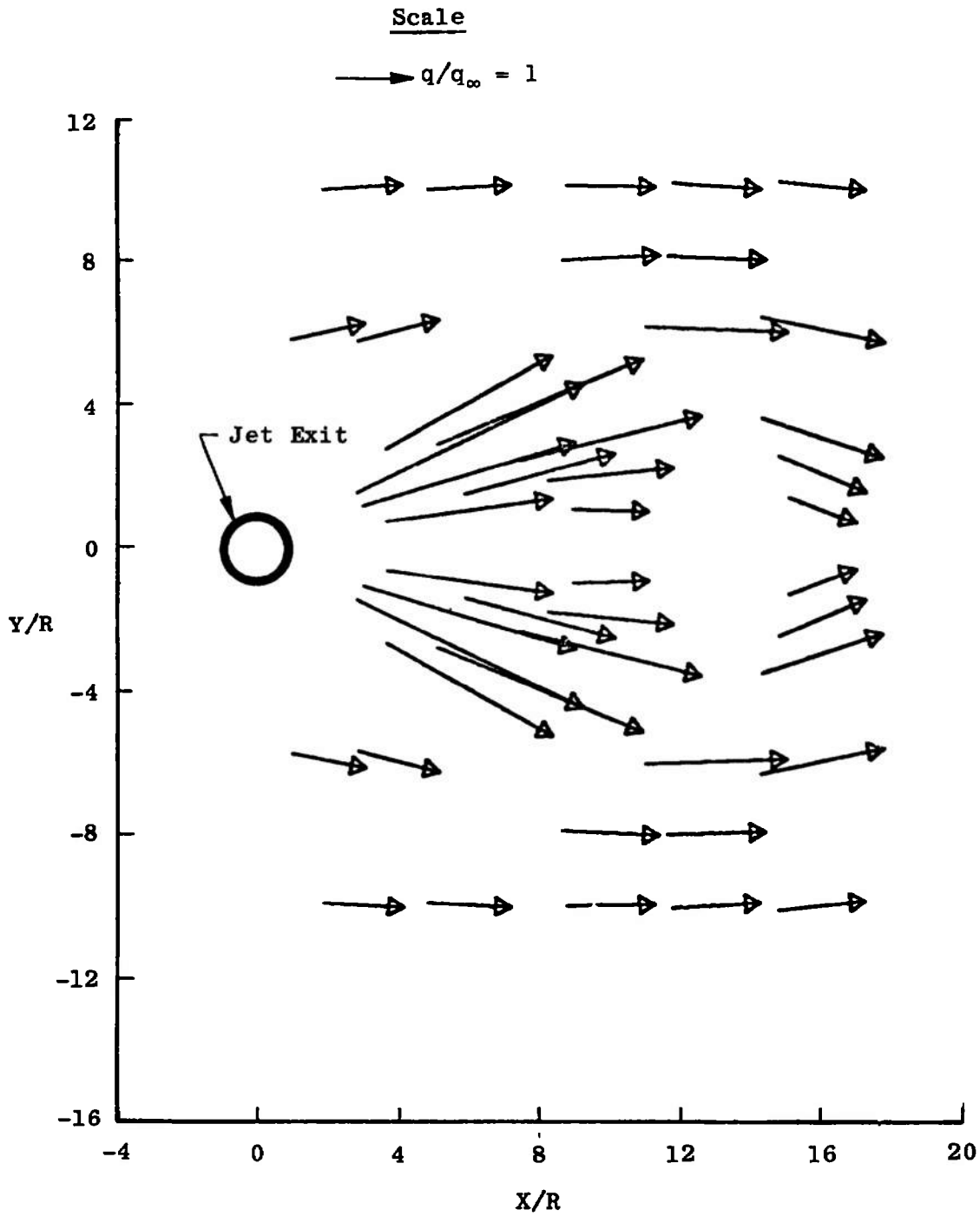

k. Z/R = 16.000
Fig. 1 Continued

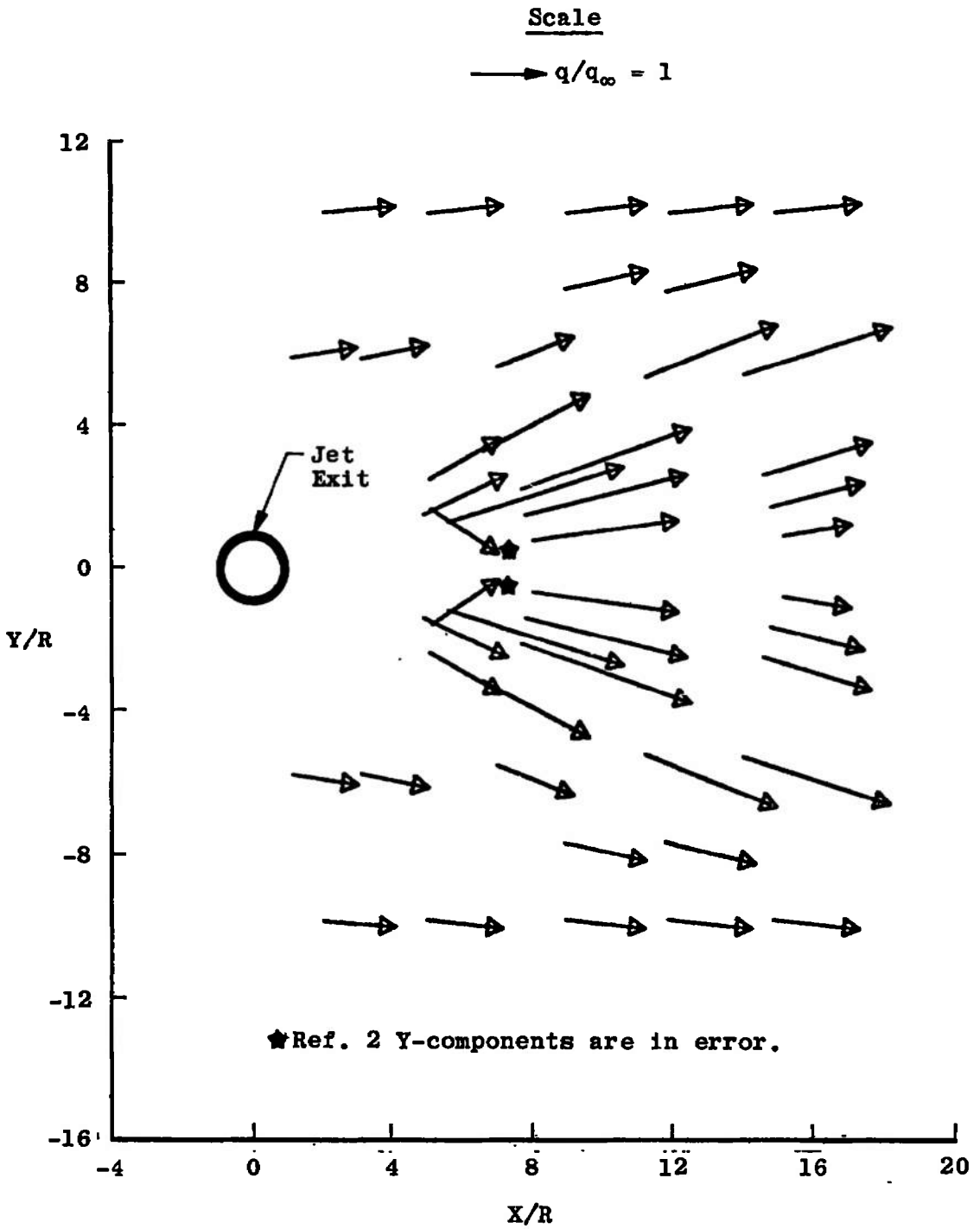

l. Z/R = 20.000
Fig. 1 Continued

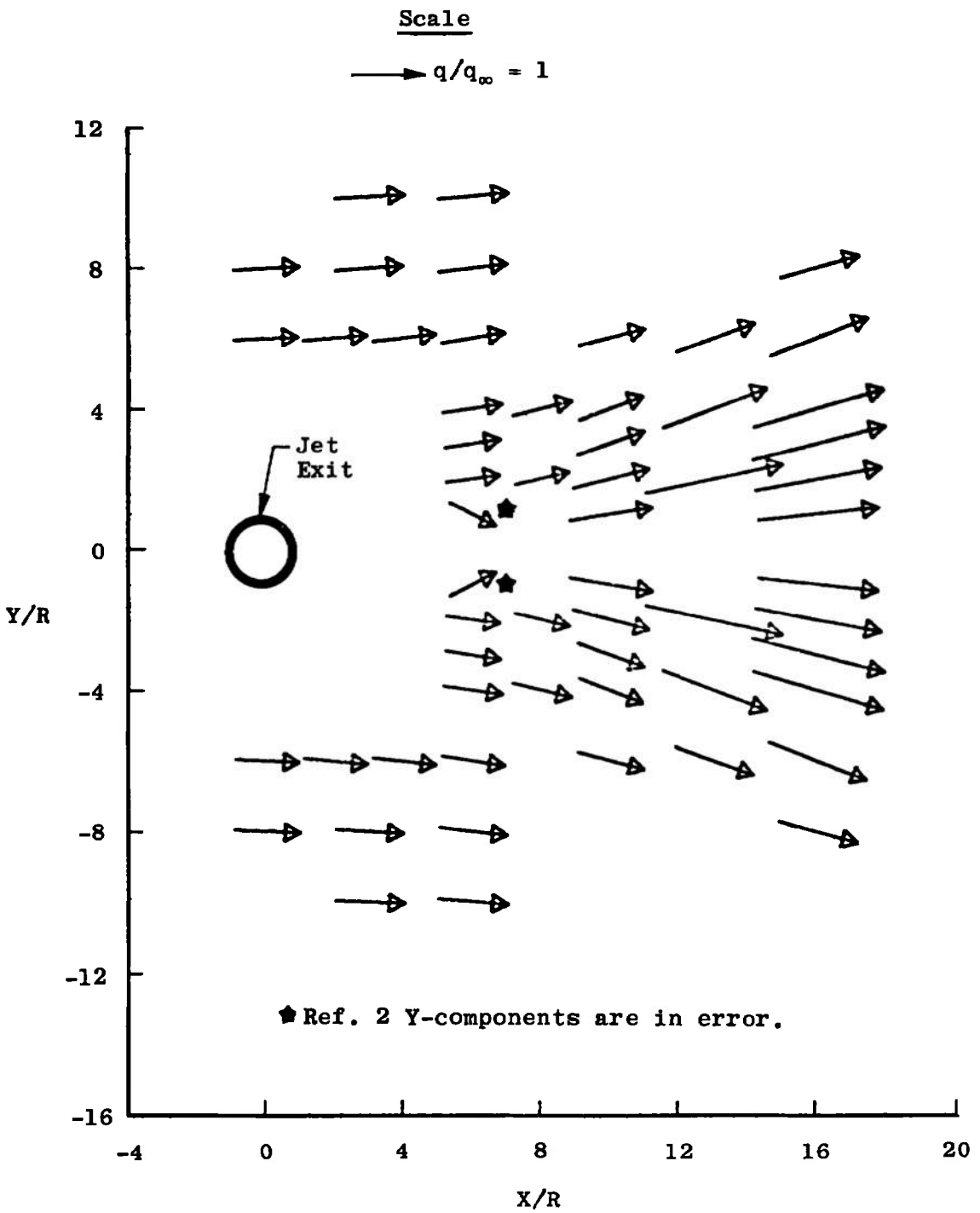

m. Z/R = 24.000
Fig. 1 Concluded

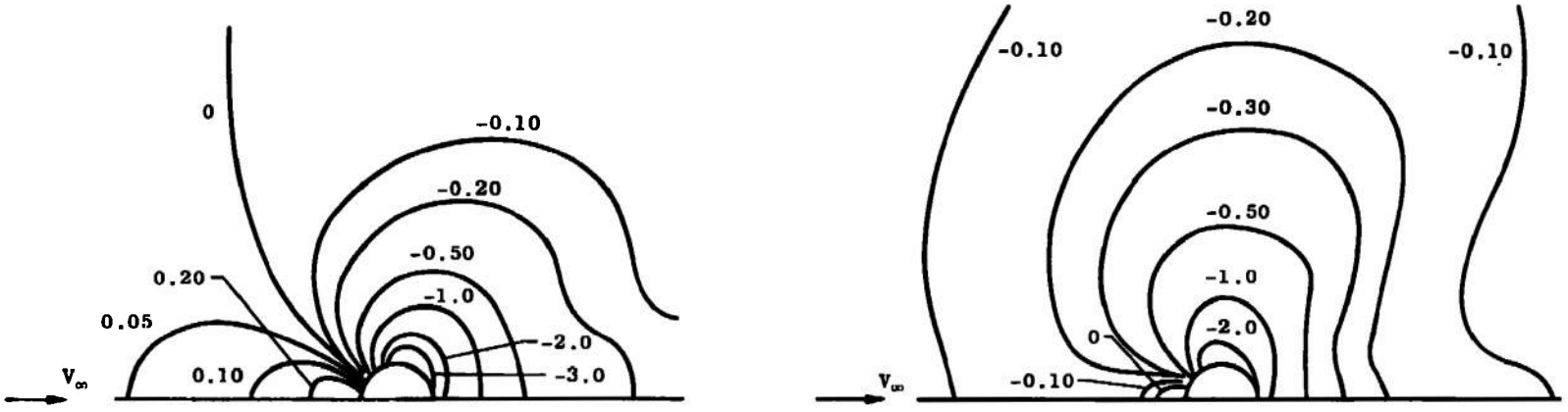

a. $V_j/V_\infty = 4.0$

b. $V_j/V_\infty = 8.0$

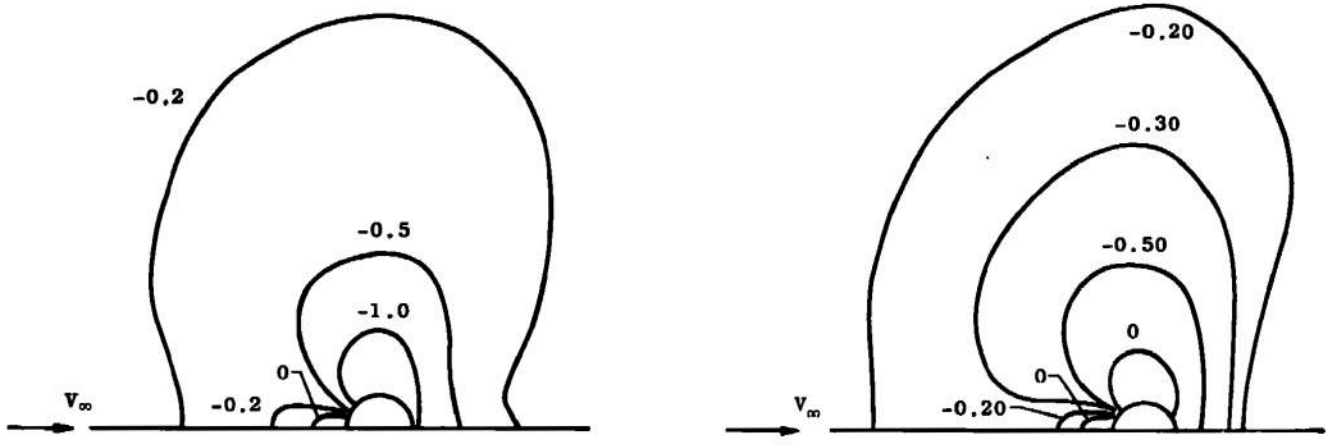

c. $V_j/V_\infty = 10.0$

d. $V_j/V_\infty = 12.0$

Fig. 2 Typical Flat-Plate Pressure Coefficient Contours (Ref. 2)

a. Oil-Trace Photograph (Ref. 2)
Fig. 3 Flat-Plate Studies, $V_i/V_\infty = 8.0$

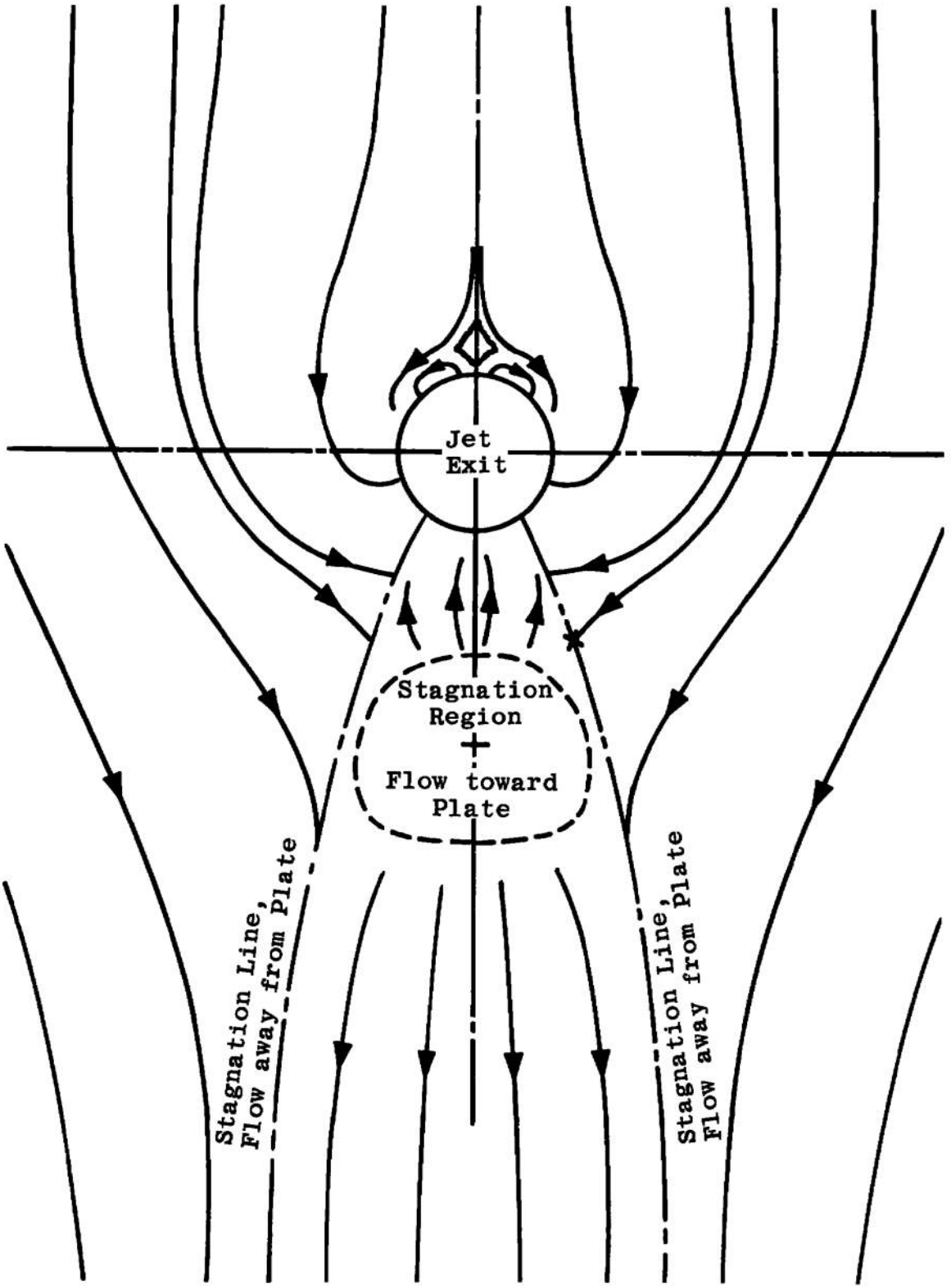

b. Authors' Interpretation of Streamlines
Fig. 3 Concluded

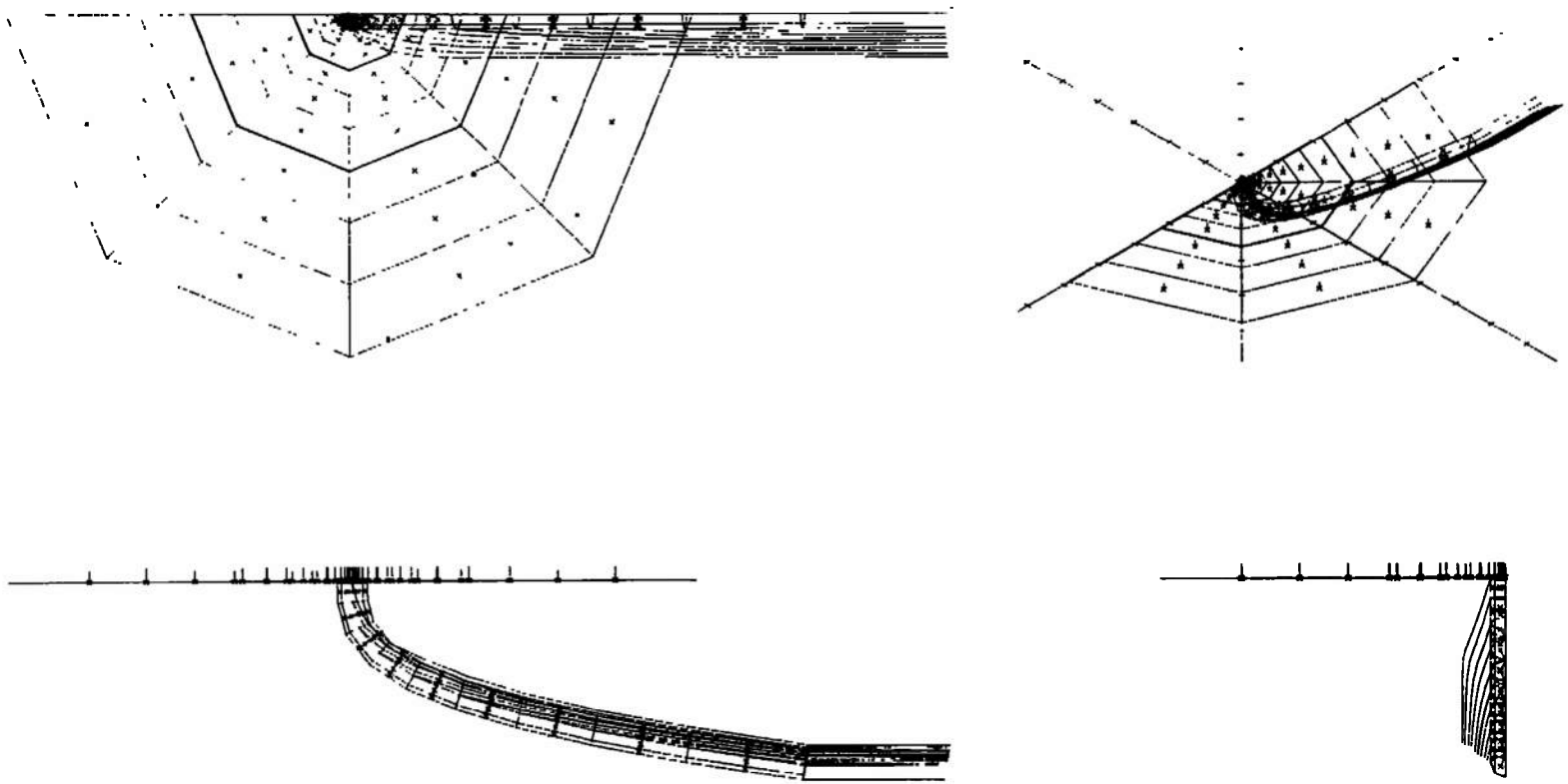

Fig. 4 Vortex-Lattice Model of a Jet Exhausting from a Flat Plate into a Crossflow, $V_j/V_\infty = 2.145$

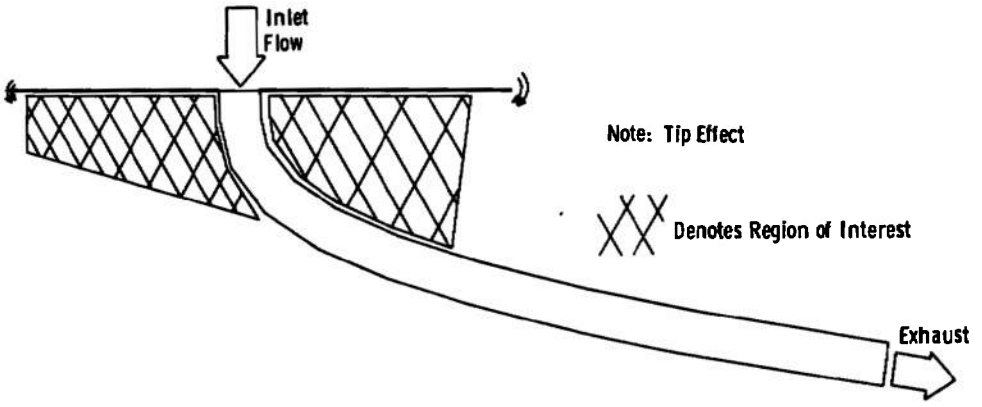

a. Grid Plate, Flow through Tube

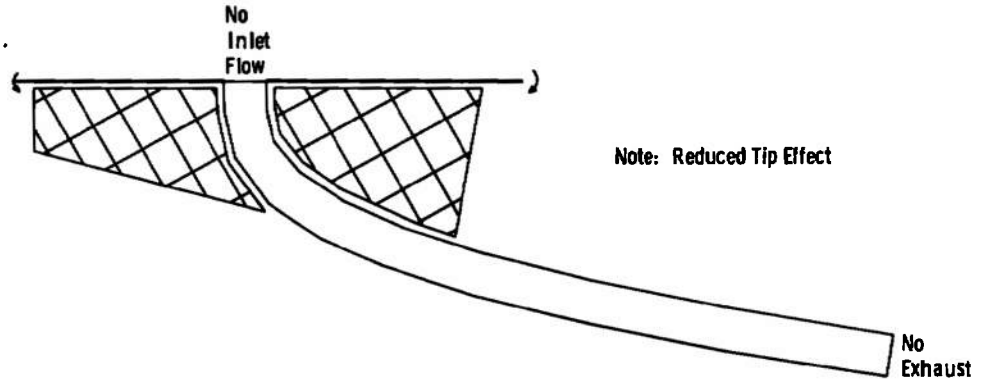

b. Grid Plate, No Flow through Tube

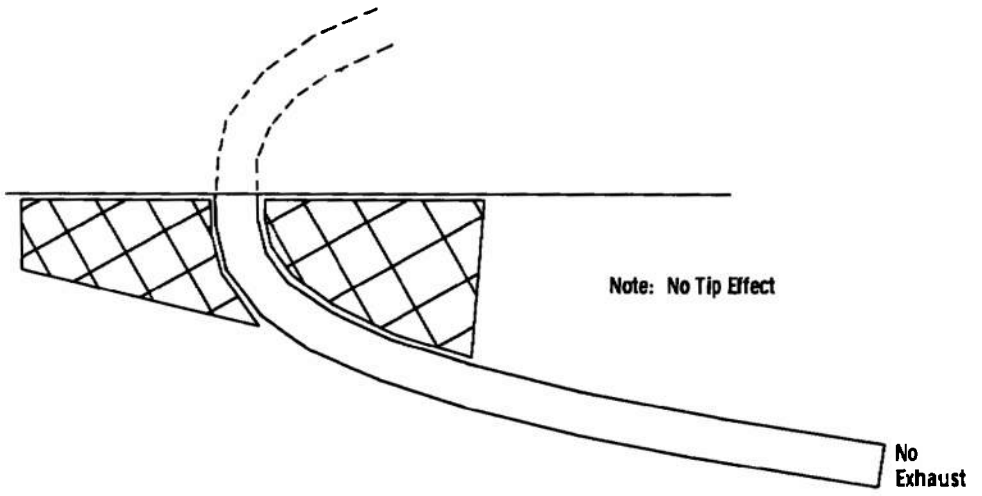

c. Symmetry Plane, No Flow through Tube

Fig. 5 Jet Exhausting from a Flat Plate

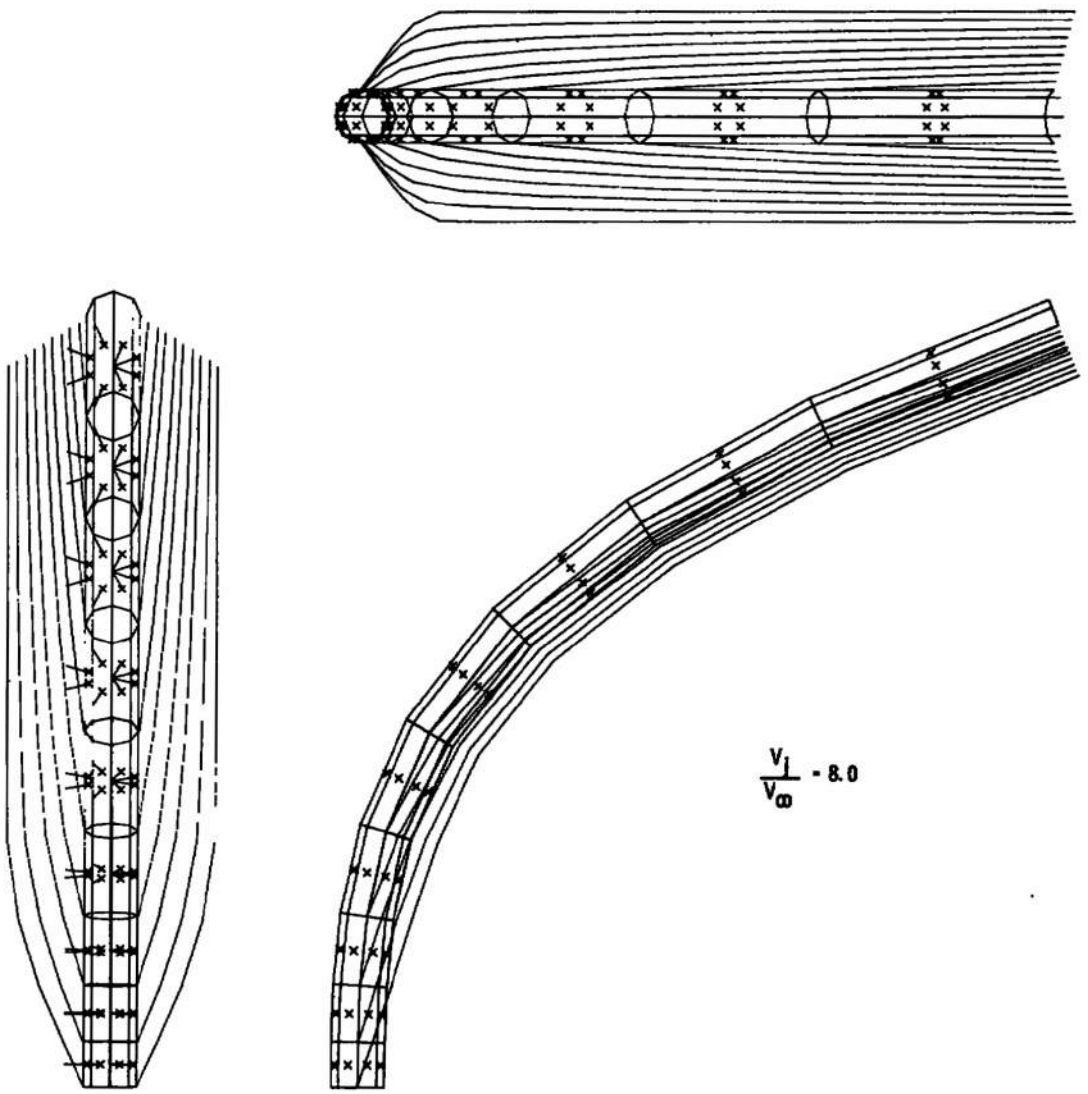

Fig. 6 Model 1.x000

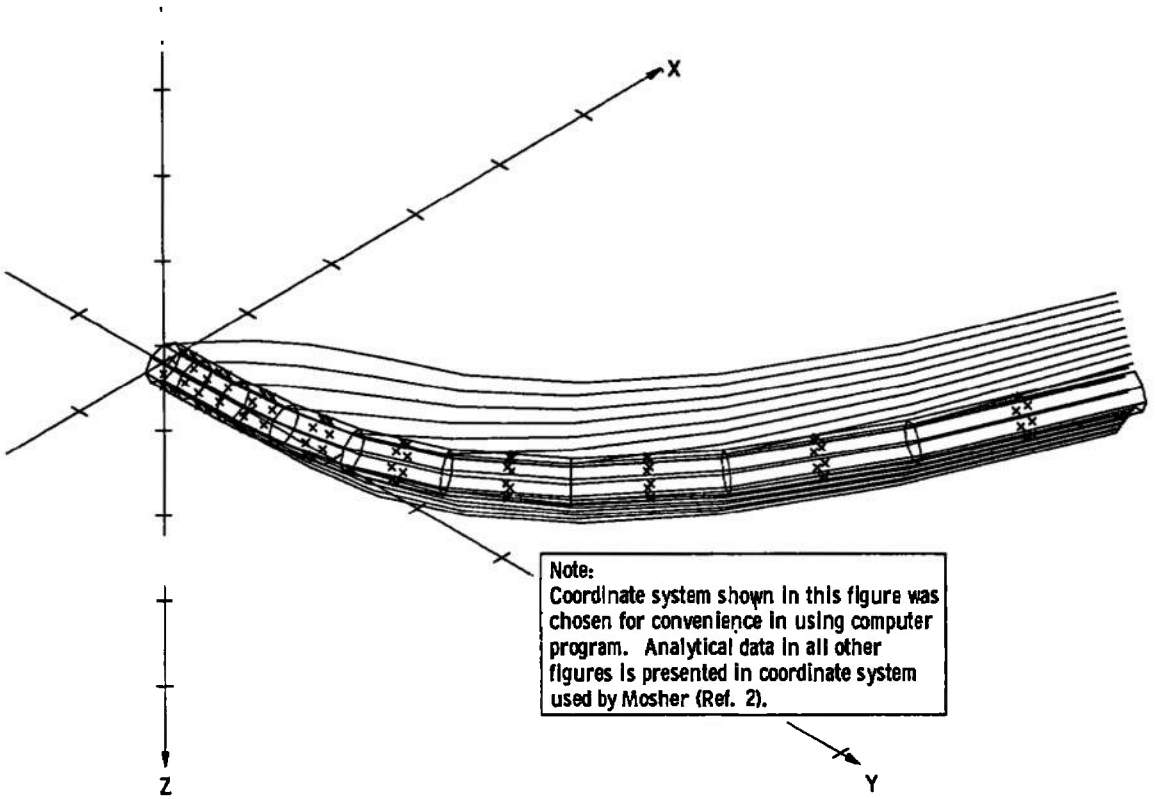

Fig. 6 Concluded

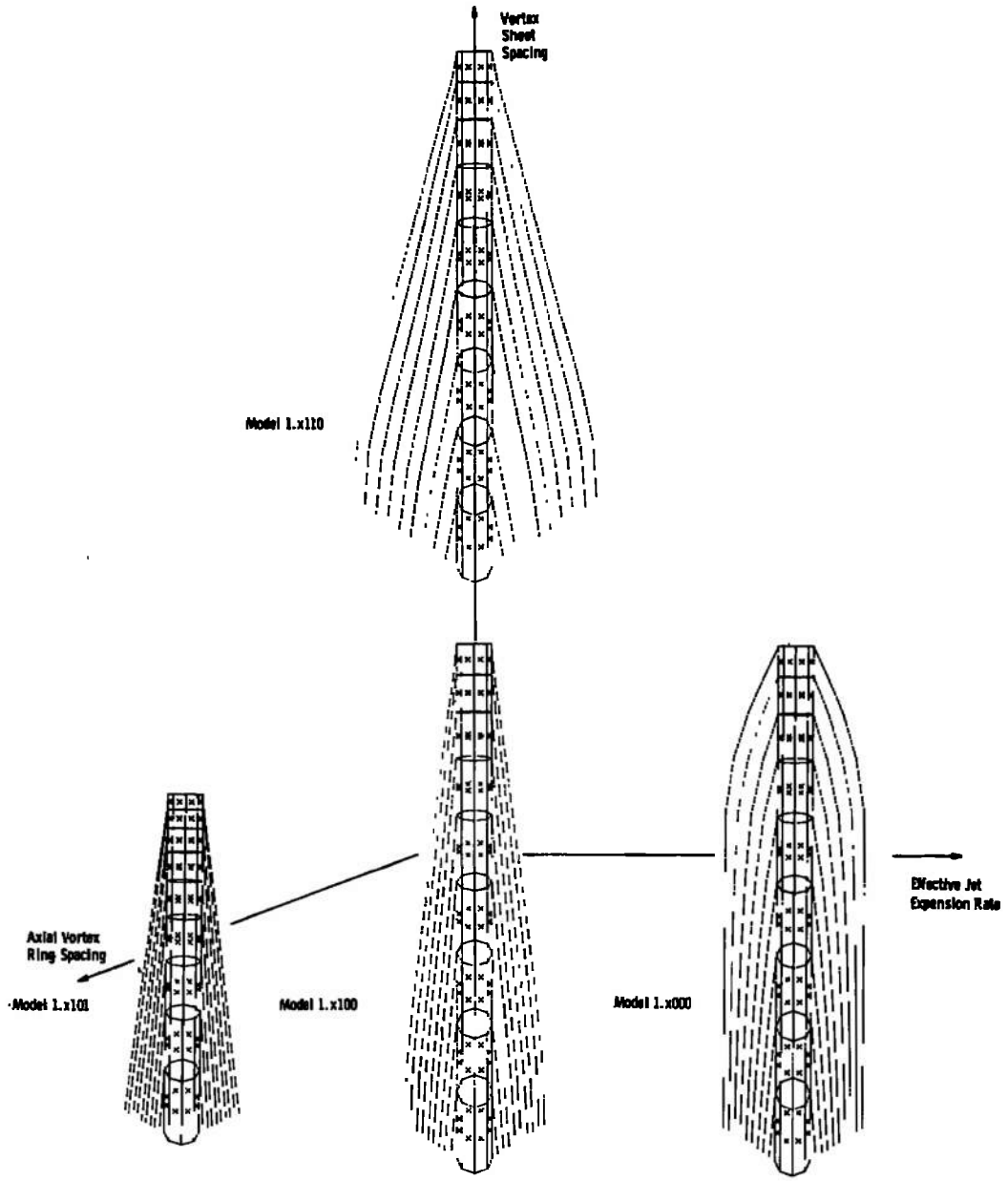

Fig. 7 Definition of Variable Parameters

Point	X/R	Y/R	Z/R	q/q_∞	
				1.0000	1.3000
1	6	1	24	1.535	2.329
2	6	6	24	1.217	2.487
3	6	10	24	0.972	2.031
4	6	2	10	5.063	43.25
5	6	10	12	0.516	6.838
6	6	6	5	1.049	9.573
7	6	10	5	0.753	4.580

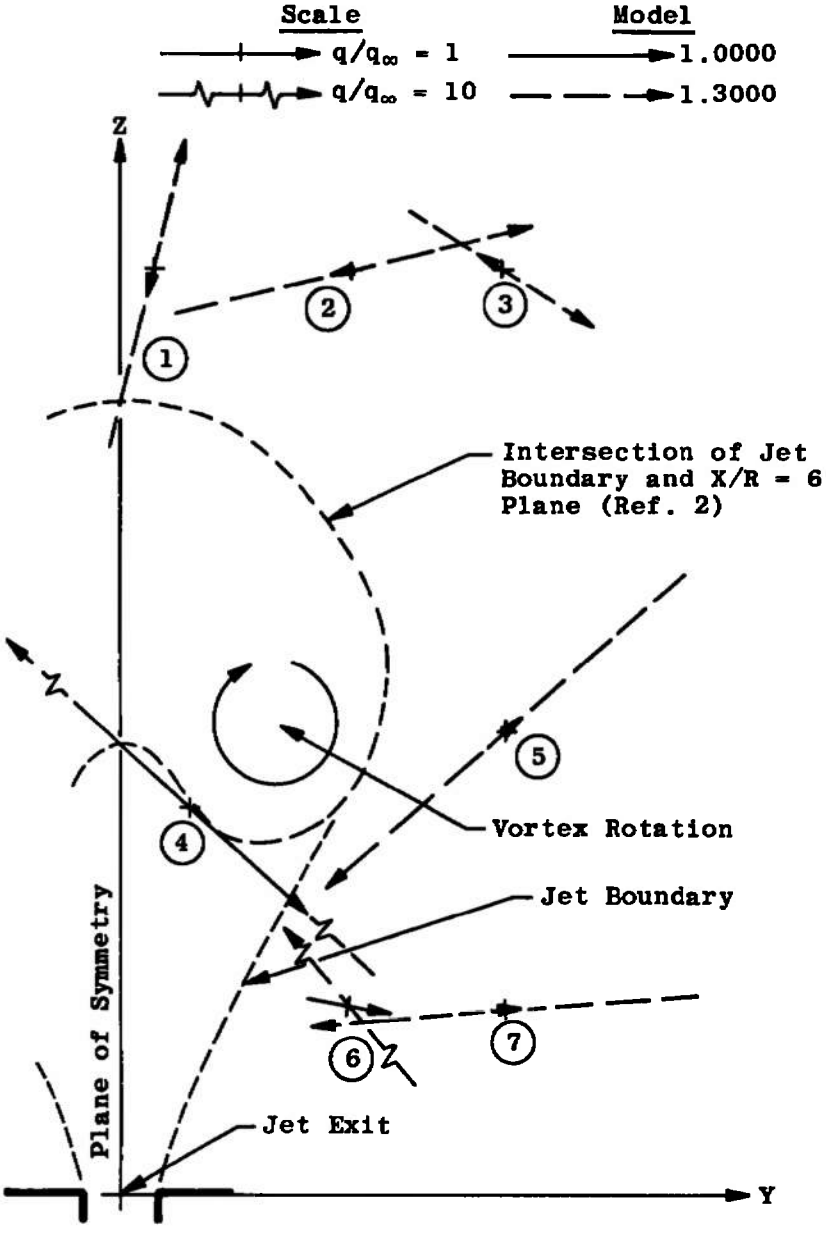

a. X/R = 6

Fig. 8 Comparisons of Analytical q-Vector Projections from Models 1.0000 and 1.3000

Point	X/R	Y/R	Z/R	q/q_∞	
				1.0000	1.3000
1	6	10	24	0.972	2.031
2	6	10	12	0.605	6.838
3	3	10	5	0.596	5.598
4	10	10	5	0.949	2.670
5	16	10	5	1.044	1.357

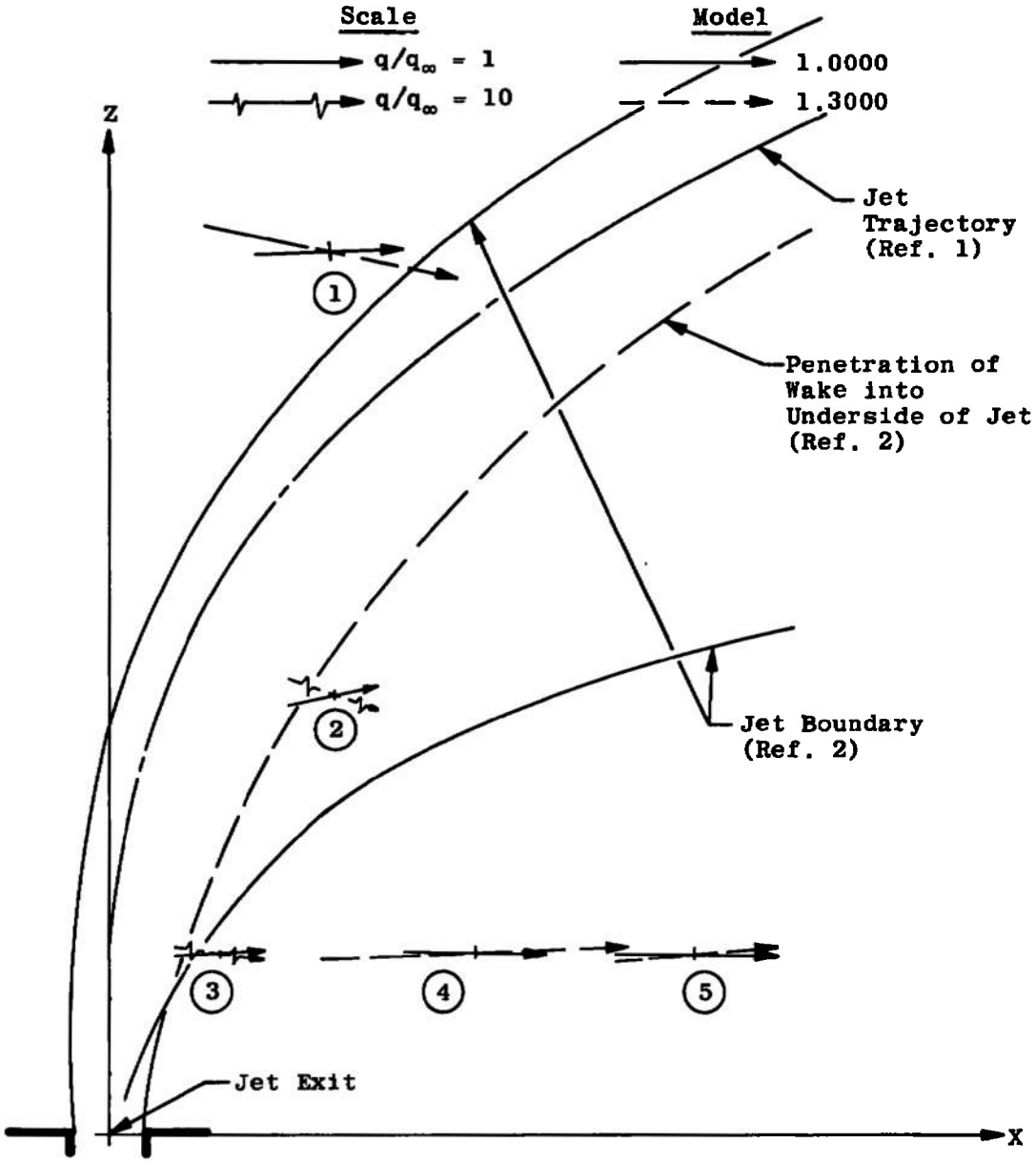

b. Y/R = 10

Fig. 8 Continued

Point	X/R	Y/R	Z/R	q/q_∞	
				1.0000	1.3000
1	3	10	5	0.596	5.598
2	10	10	5	0.949	2.670
3	16	10	5	1.044	1.357
4	0	8	5	0.556	7.640
5	6	6	5	1.049	9.573
6	13	6	5	1.164	1.348

Scale

$q/q_\infty = 1$

$q/q_\infty = 10$

Model

1.0000

1.3000

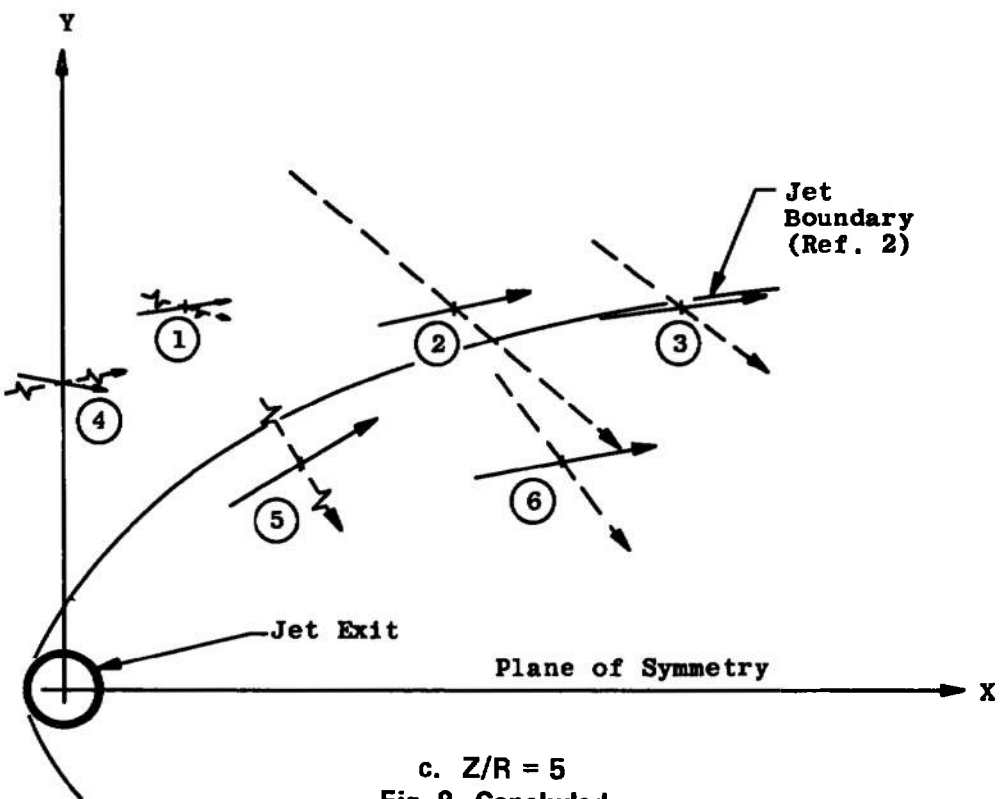

c. Z/R = 5

Fig. 8 Concluded

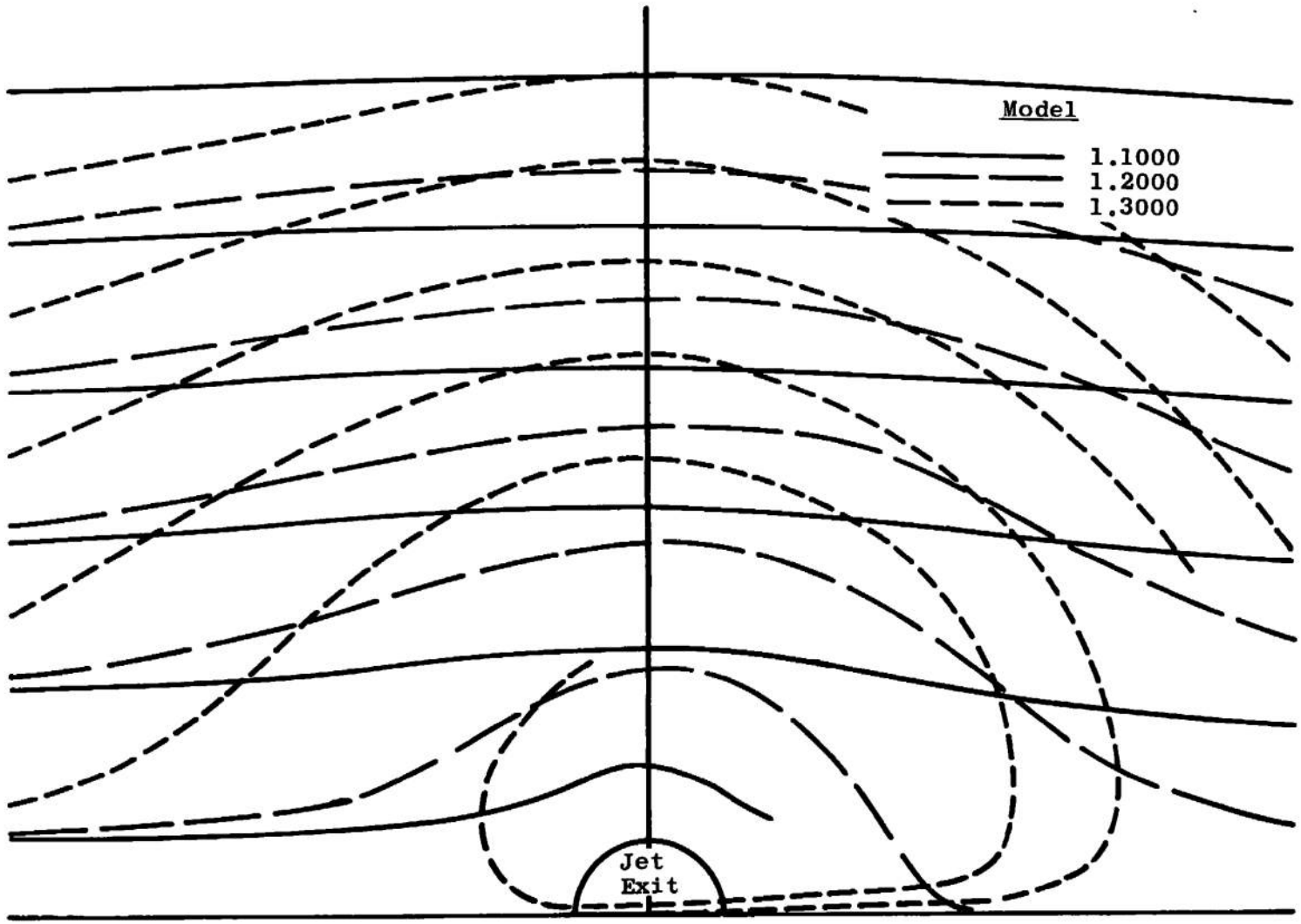

Fig. 9 Comparison of Computed Streamlines for Models 1.1000, 1.2000, and 1.3000

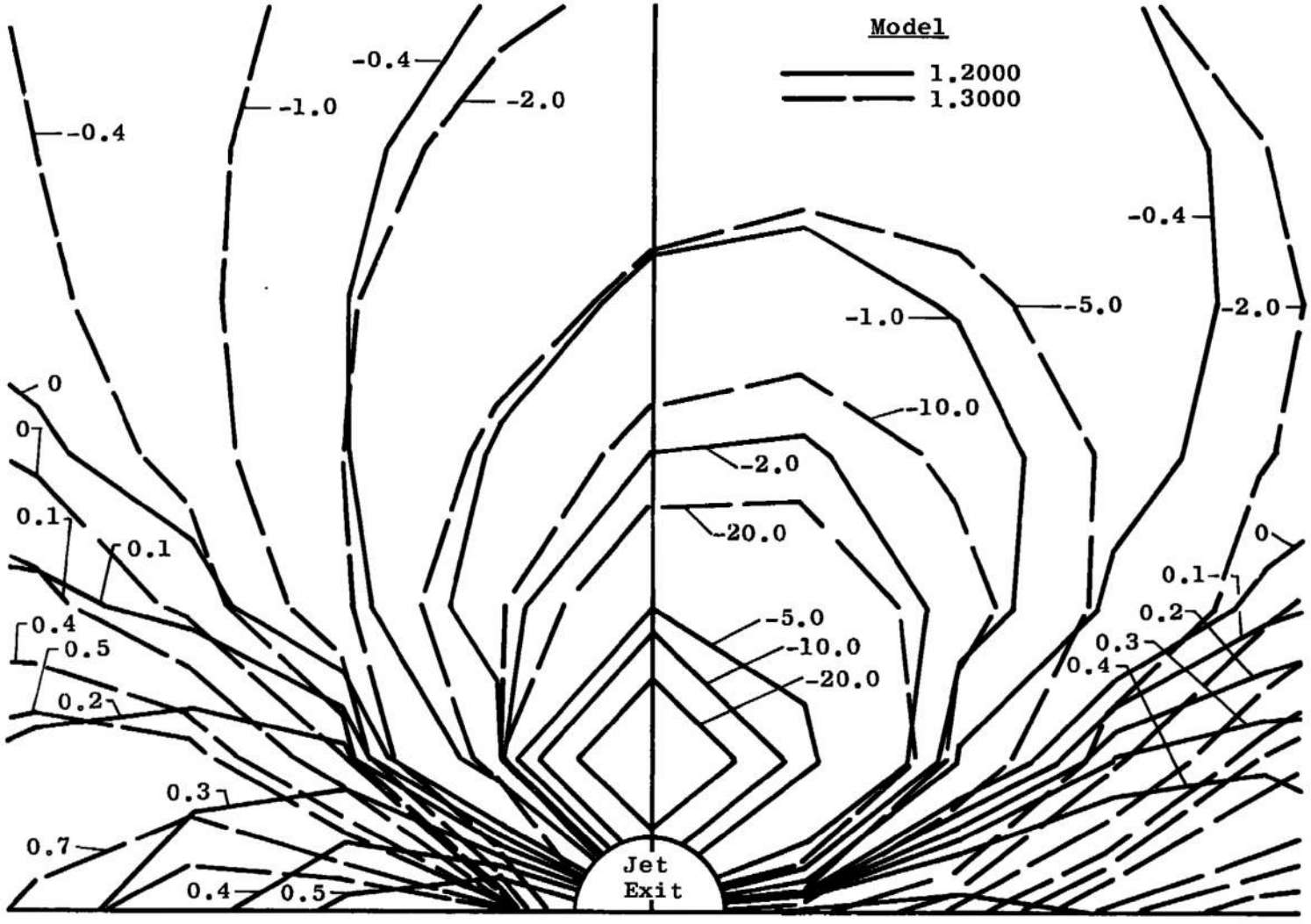

Fig. 10 Comparison of Computed Pressure Coefficient Contours for Models 1.2000 and 1.3000

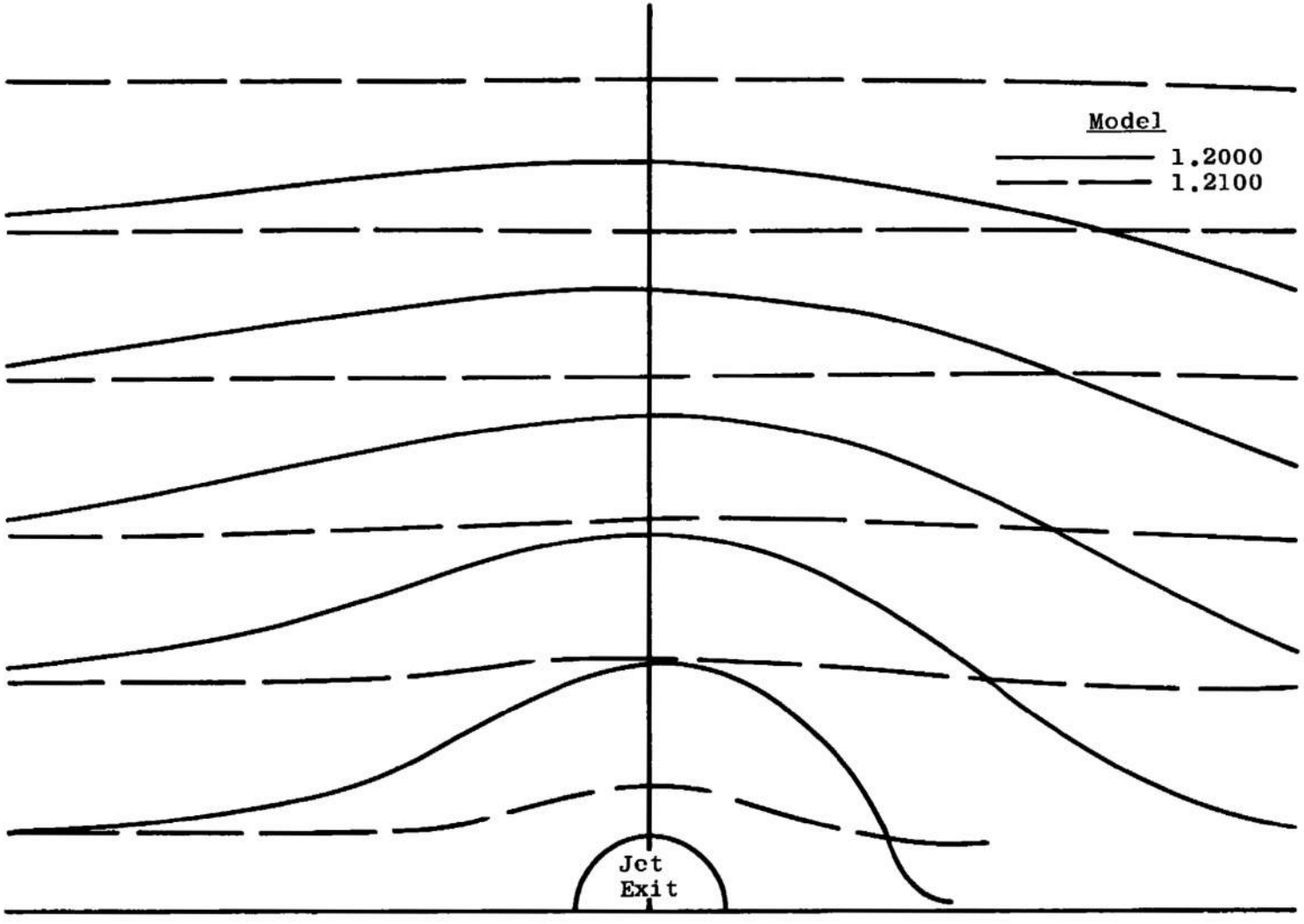

Fig. 11 Comparison of Computed Streamlines for Models 1.2000 and 1.2100

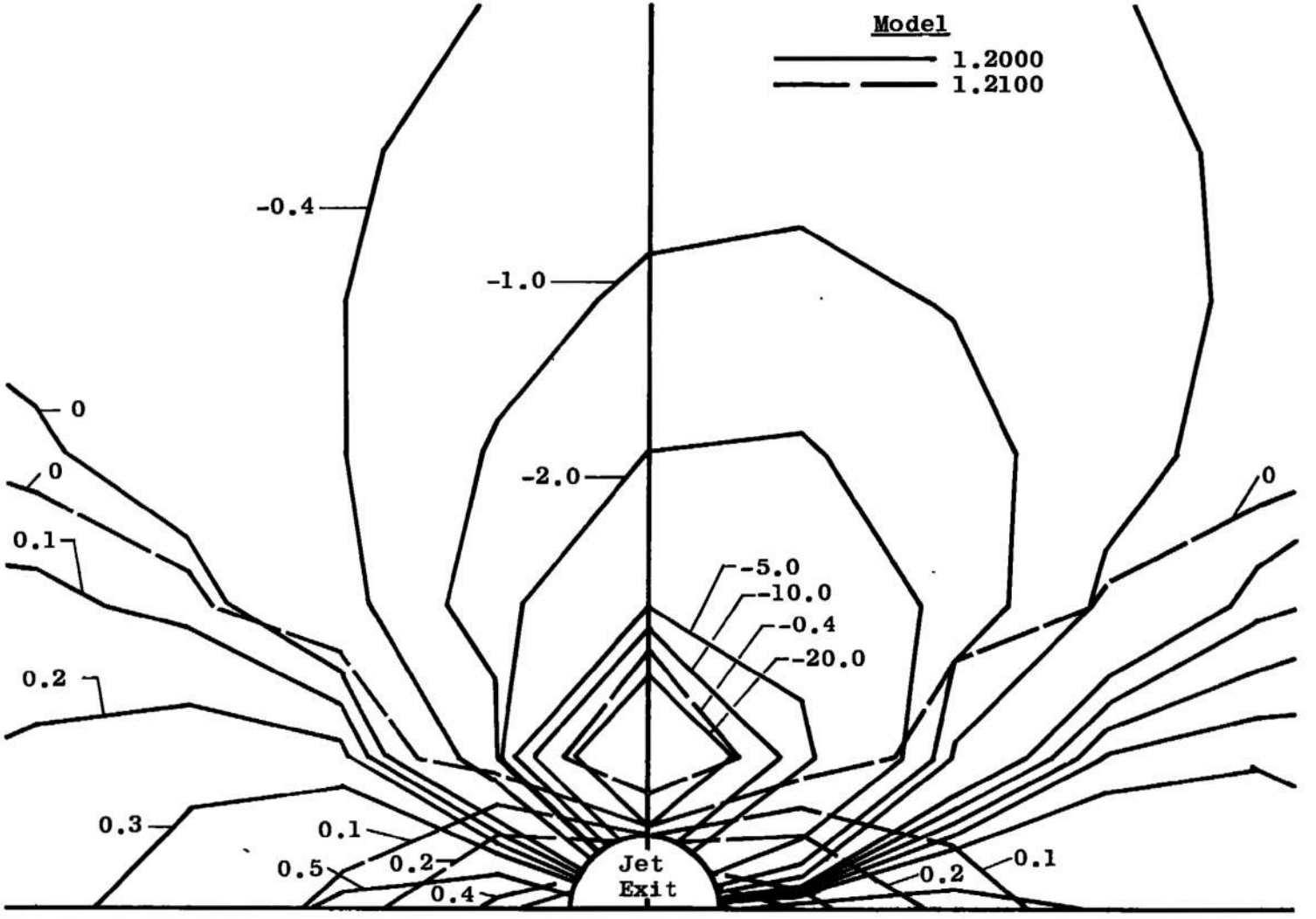

Fig. 12 Comparison of Computed Pressure Coefficient Contours for Models 1.2000 and 1.2100

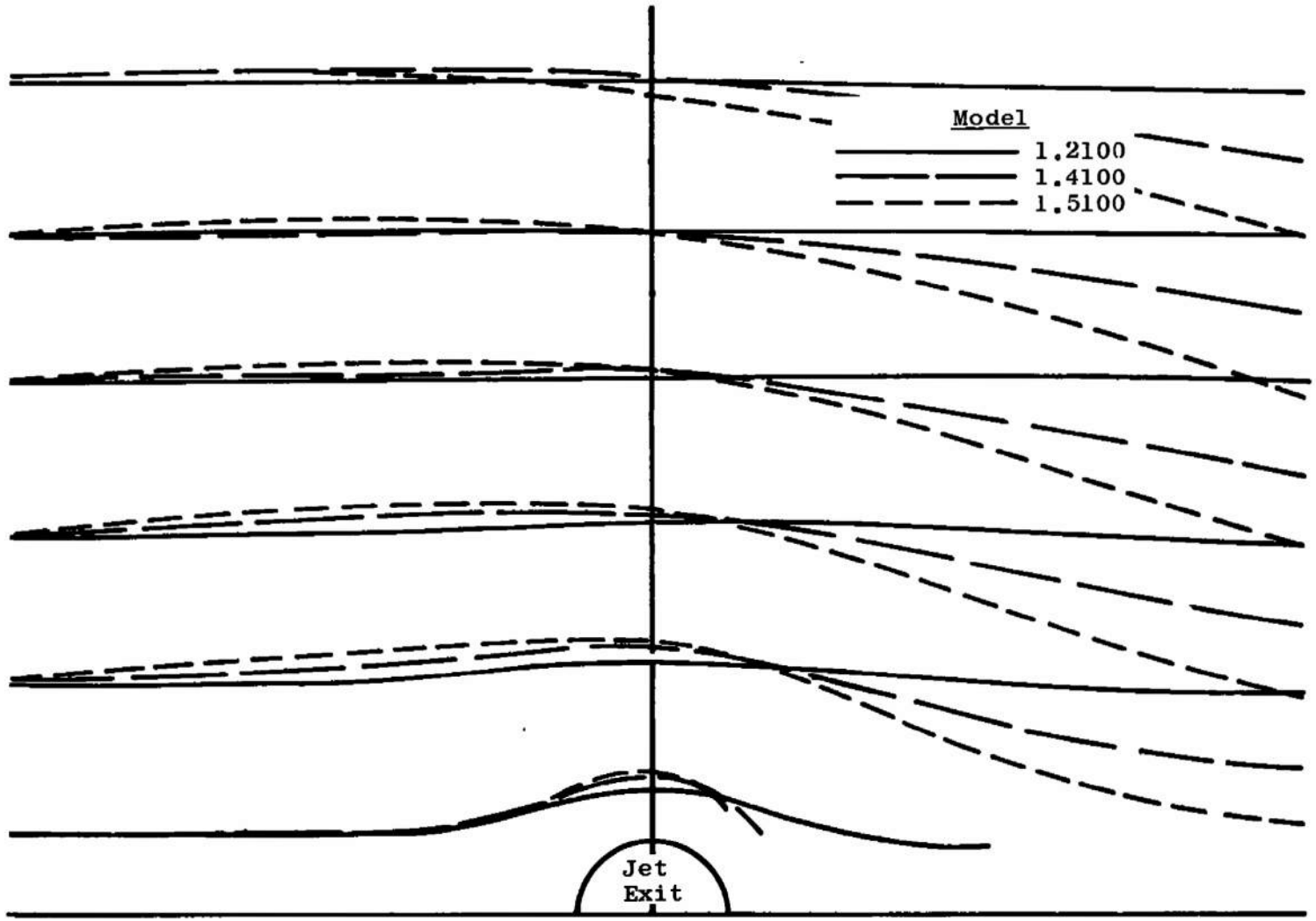

Fig. 13 Comparison of Computed Streamlines for Models 1.2100, 1.4100, and 1.5100

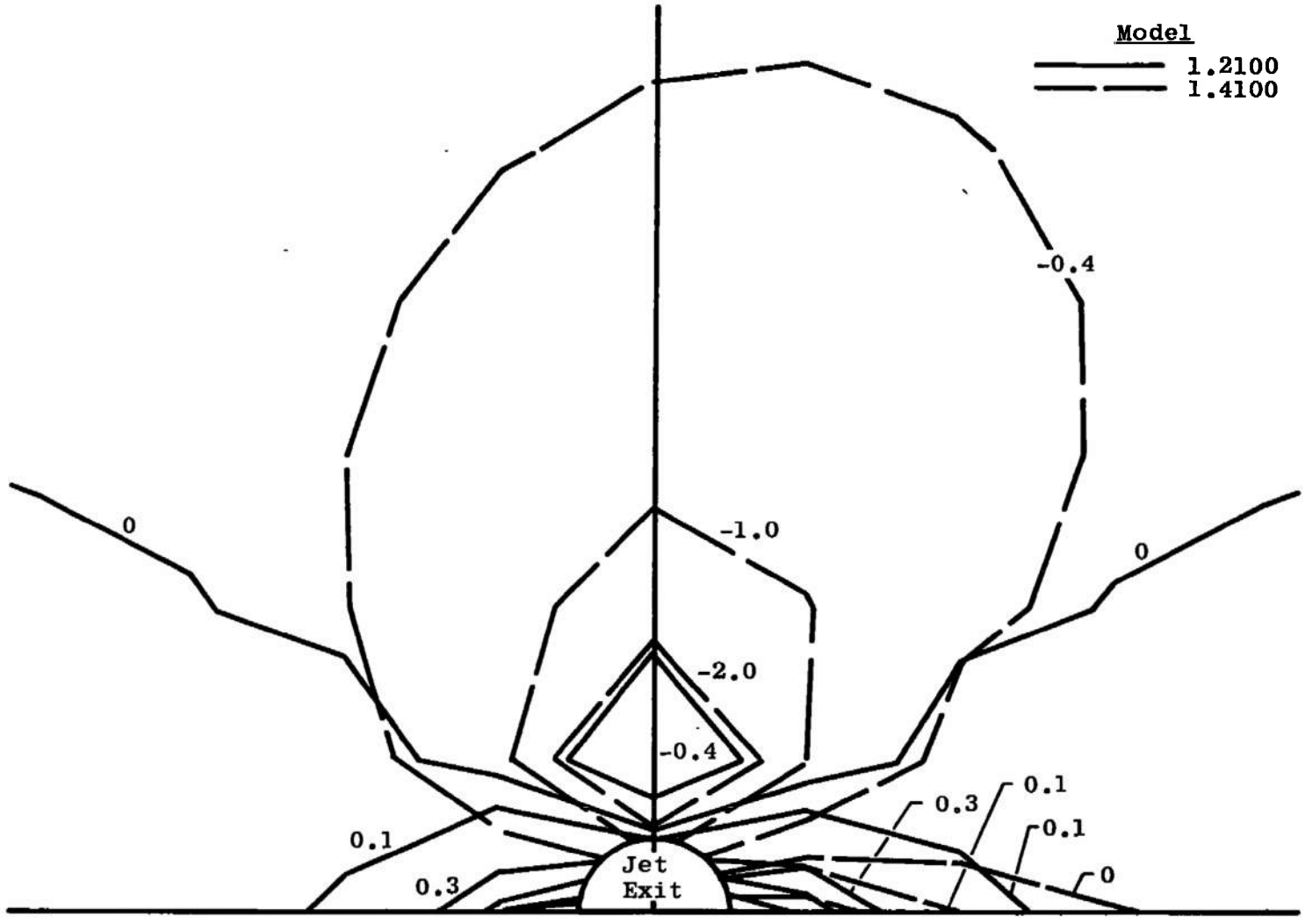

Fig. 14 Comparison of Computed Pressure Coefficient Contours for Models 1.2100 and 1.4100

Point	X/R	Y/R	Z/R	q/q_∞	
				1.4100	1.5100
1	6	1	24	0.634	3.389
2	6	6	24	1.173	2.375
3	6	10	24	1.214	1.695
4	6	2	10	1.863	6.136
5	6	10	12	1.740	2.822
6	6	6	5	1.481	2.250
7	6	10	5	1.416	1.977

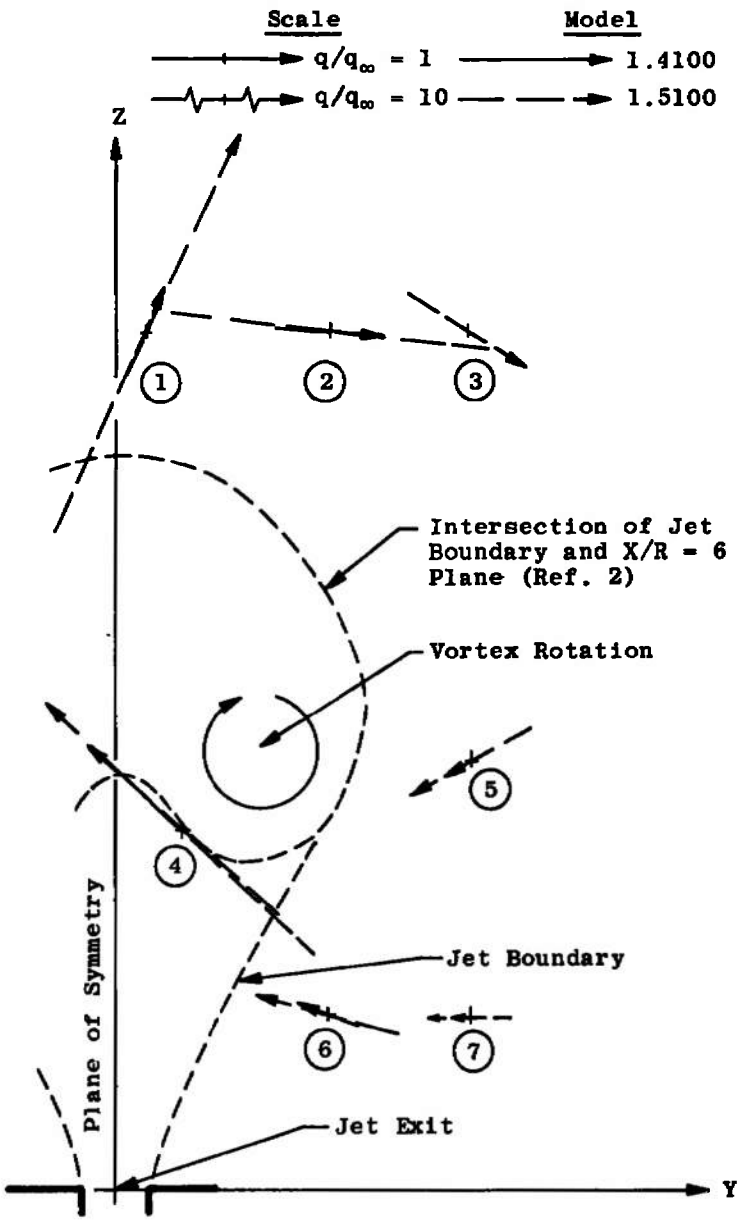

a. X/R = 6

Fig. 15 Comparison of Analytical q-Vector Projections from Models 1.4100 and 1.5100

Point	X/R	Y/R	Z/R	q/q_∞	
				1.4100	1.5100
1	6	10	24	1.214	1.695
2	6	10	12	1.740	2.789
3	3	10	5	1.506	2.146
4	10	10	5	1.268	1.659
5	16	10	5	1.121	1.327

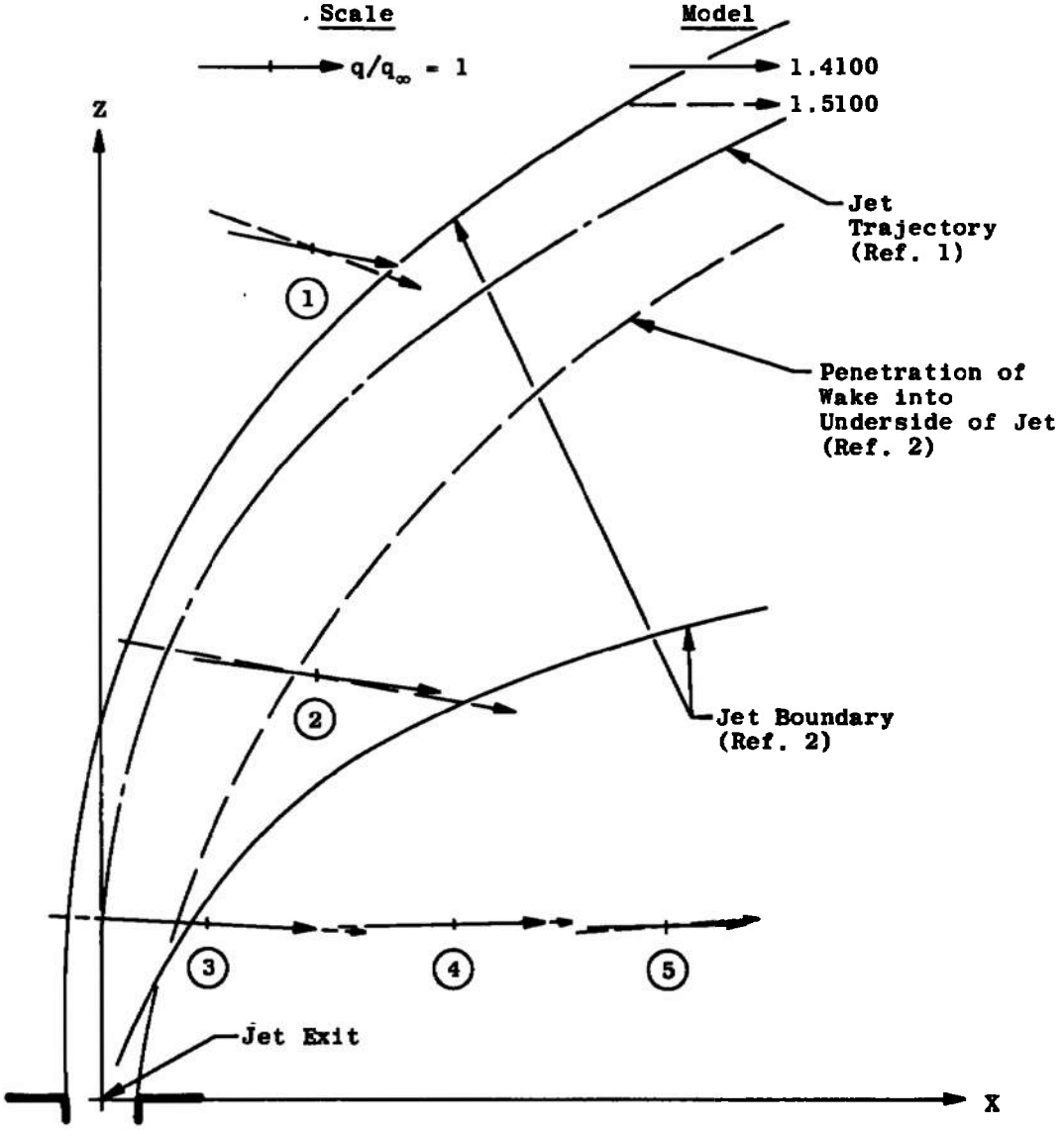

b. Y/R = 10

Fig. 15 Continued

Point	X/R	Y/R	Z/R	q/q_∞	
				1.4100	1.5100
1	3	10	5	1.506	2.146
2	10	10	5	1.268	1.659
3	16	10	5	1.121	1.327
4	0	8	5	1.667	2.493
5	6	6	5	1.481	2.250
6	13	6	5	1.113	1.339

Scale

q/q_∞ = 1

Model

1.4100

1.5100

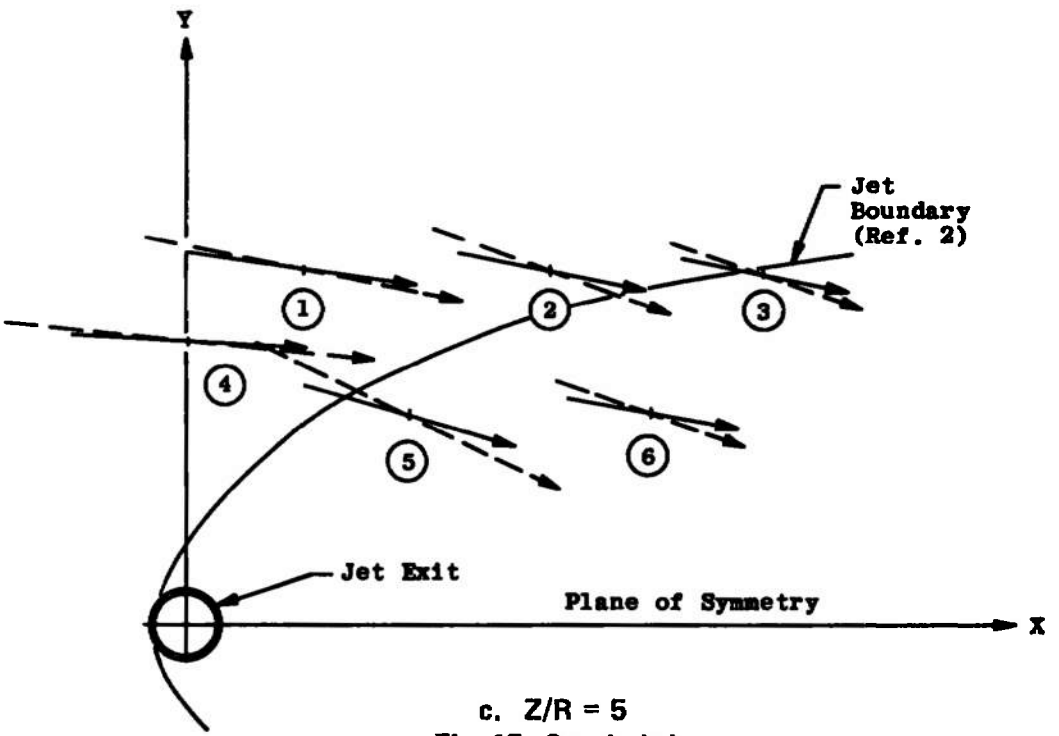

c. Z/R = 5

Fig. 15 Concluded

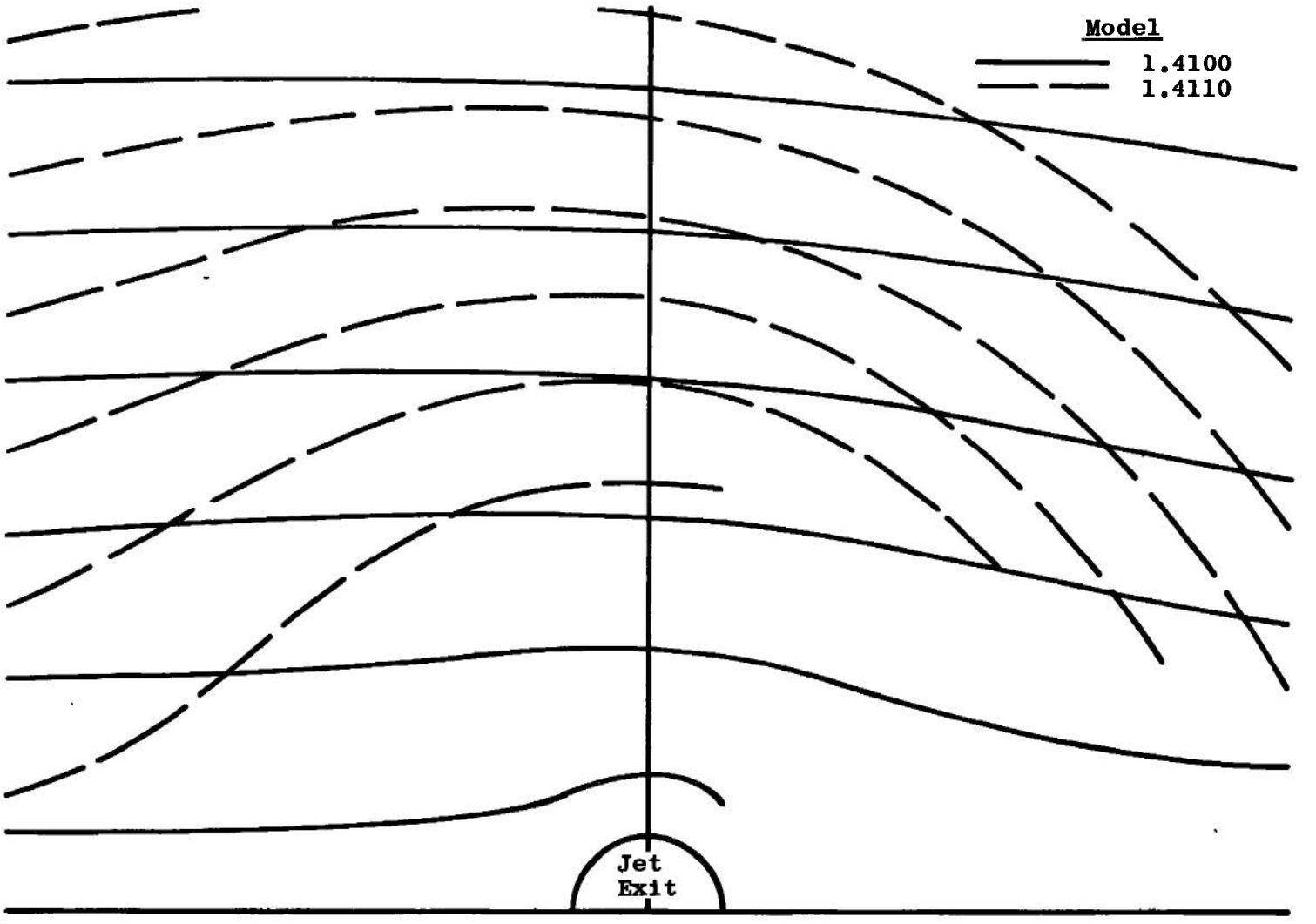

Fig. 16 Comparison of Computed Streamlines for Models 1.4100 and 1.4110

Point	X/R	Y/R	Z/R	q/q_∞	
				1.4100	1.4110
1	6	1	24	0.634	8.620
2	6	6	24	1.173	6.620
3	6	10	24	1.214	4.326
4	6	2	10	1.863	128.732
5	6	10	12	1.740	22.973
6	6	6	5	1.481	22.743
7	6	10	5	1.416	11.540

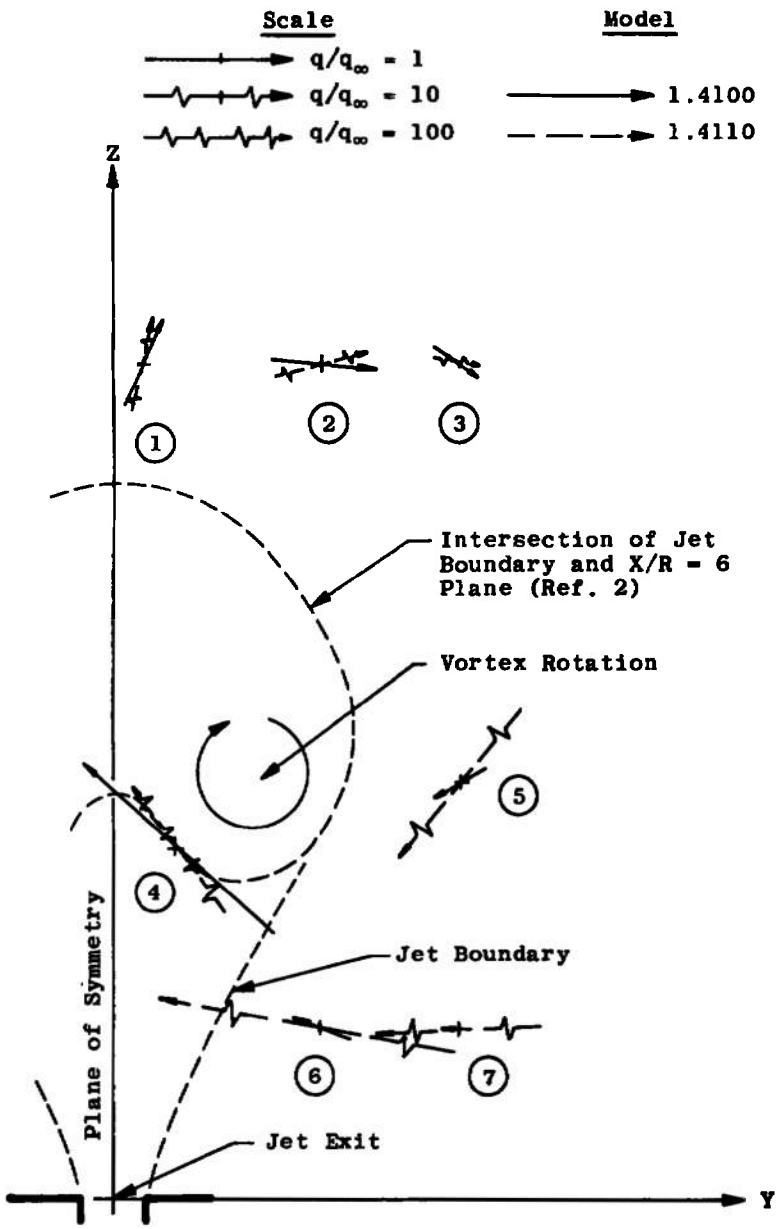

a. X/R = 6

Fig. 17 Comparison of Analytical q-Vector Projections from Models 1.4100 and 1.4110

Point	X/R	Y/R	Z/R	q/q_∞	
				1.4100	1.4110
1	6	10	24	1.214	4.326
2	6	10	12	1.740	22.973
3	3	10	5	1.506	12.411
4	10	10	5	1.268	8.117
5	16	10	5	1.121	4.666

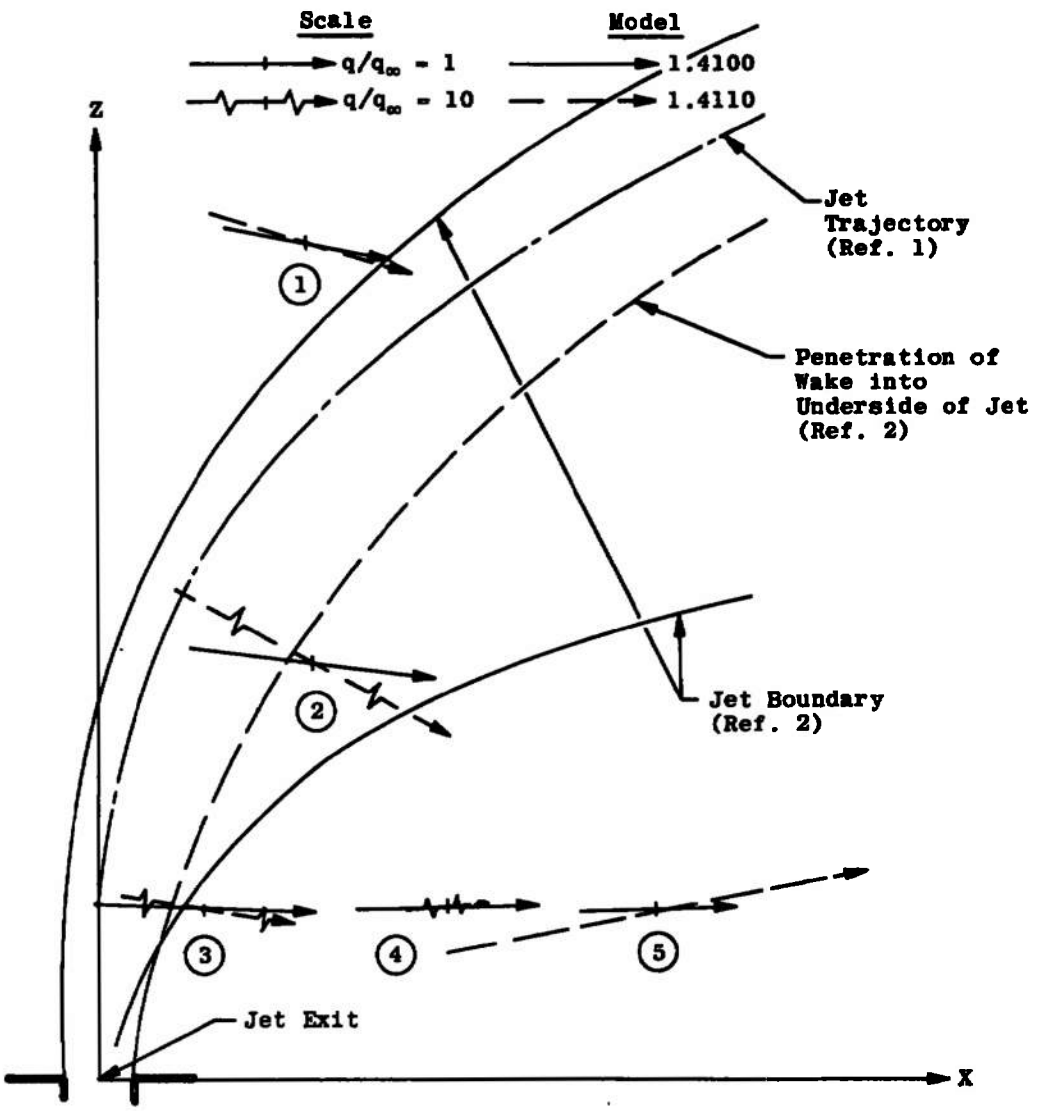

b. Y/R = 10

Fig. 17 Continued

Point	X/R	Y/R	Z/R	q/q_∞	
				1.4100	1.4110
1	3	10	5	1.506	12.412
2	10	10	5	1.268	8.117
3	16	10	5	1.121	4.666
4	0	8	5	1.667	15.785
5	6	6	5	1.481	22.743
6	13	6	5	1.113	5.355

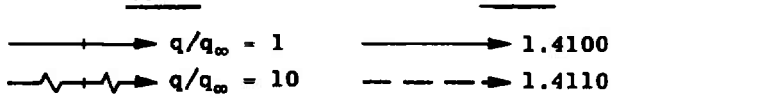

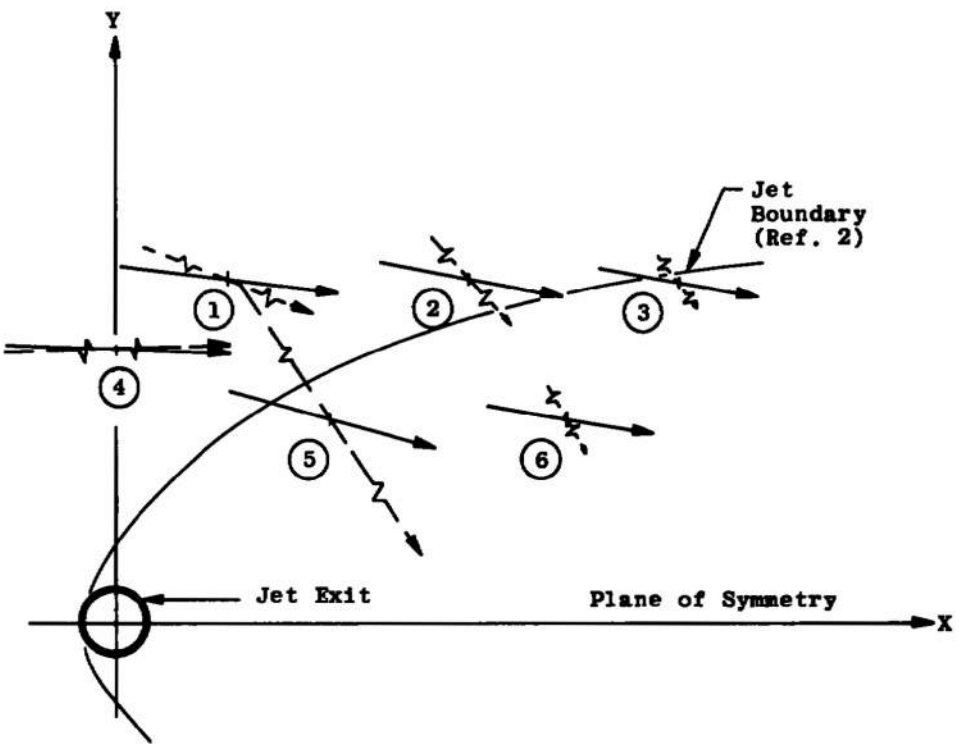

c. Z/R = 5

Fig. 17 Concluded

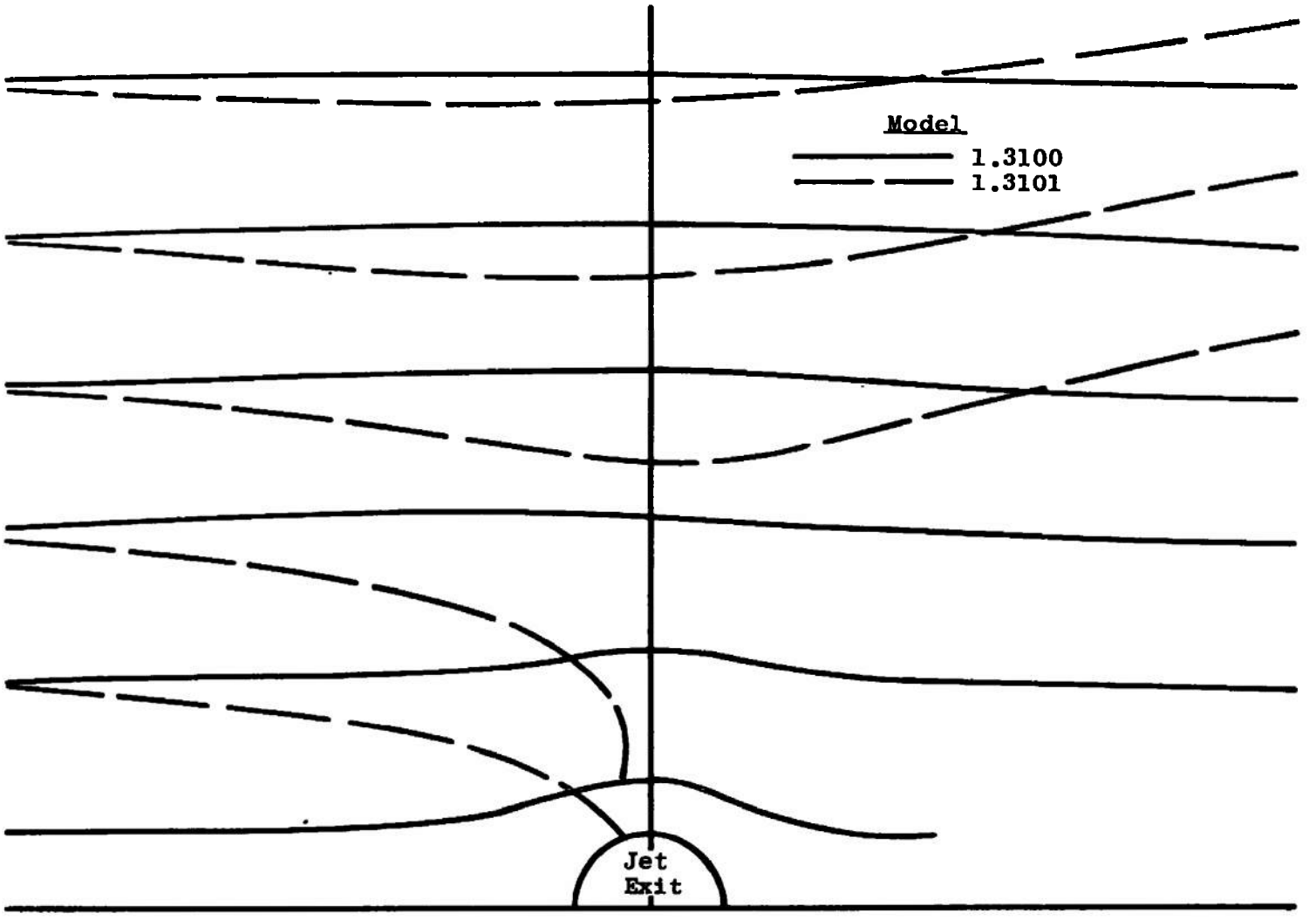

Fig. 18 Comparison of Computed Streamlines for Models 1.3100 and 1.3101

Point	X/R	Y/R	Z/R	q/q_∞
				1.3101
1	6	1	24	1.047
2	6	6	24	1.109
3	6	10	24	1.002
4	6	2	10	3.920
5	6	10	12	0.719
6	6	6	5	0.935
7	6	10	5	0.805

Scale — Model

$q/q_\infty = 1$ — 1.3101

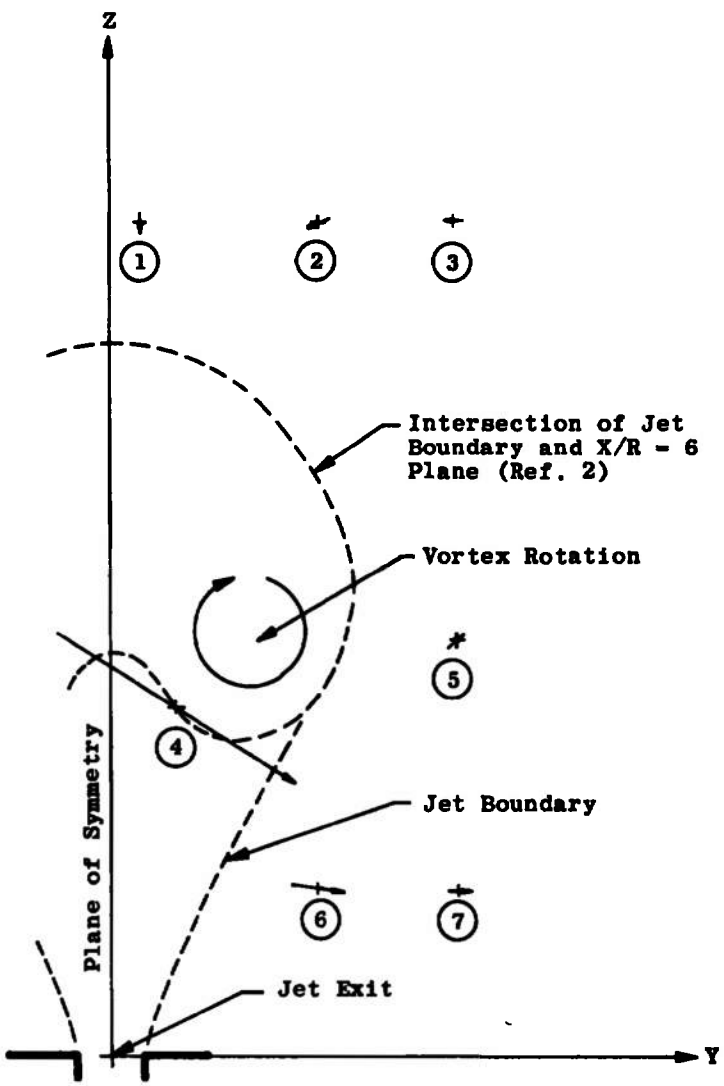

a. X/R = 6

Fig. 19 Analytical q-Vector Projections from Model 1.3101

Point	X/R	Y/R	Z/R	q/q_∞
				1.3101
1	6	10	24	1.002
2	6	10	12	0.719
3	3	10	5	0.692
4	10	10	5	0.935
5	16	10	5	1.010

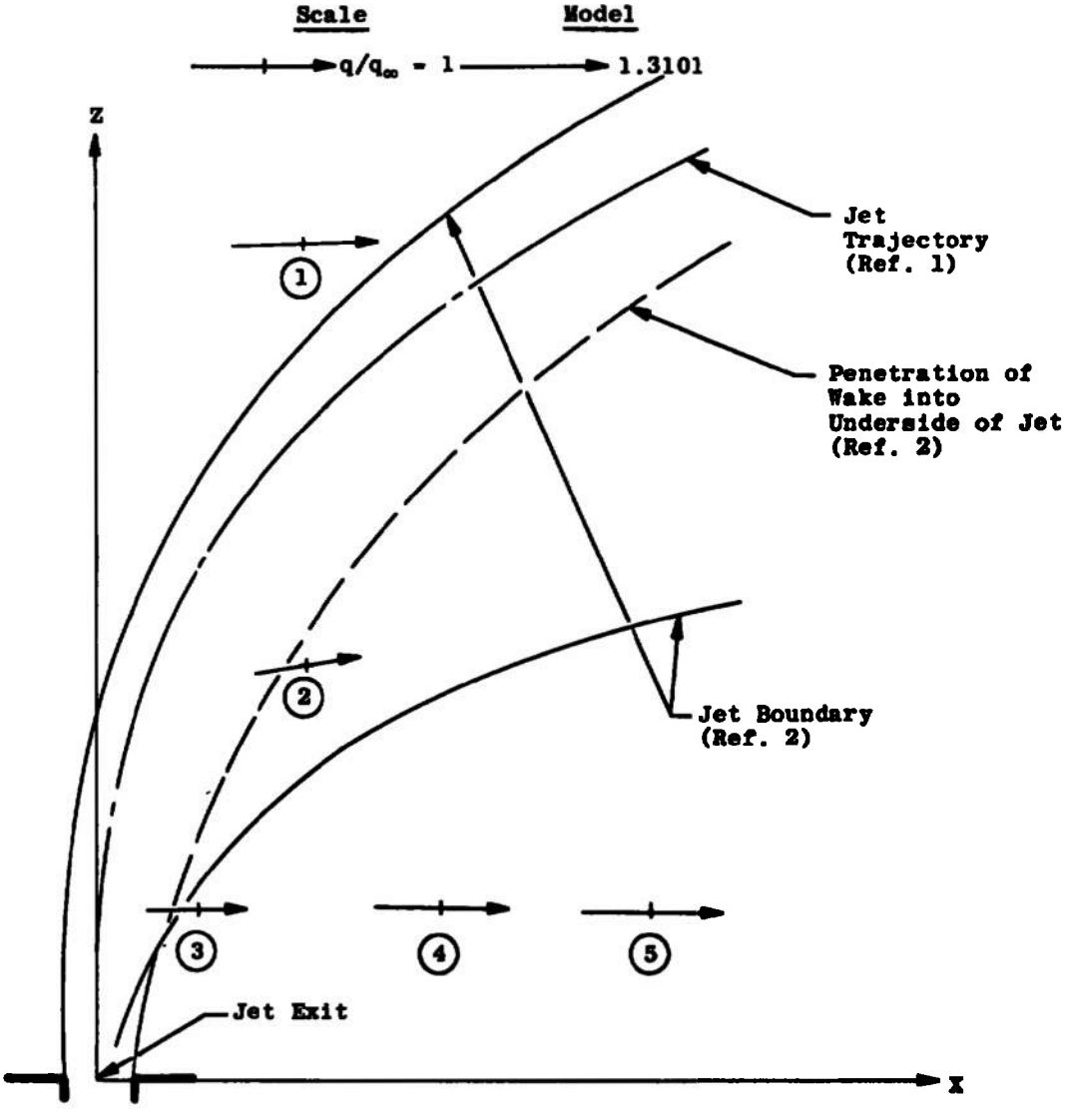

b. Y/R = 10

Fig. 19 Continued

Point	X/R	Y/R	Z/R	q/q_∞
				1.3101
1	3	10	5	0.692
2	10	10	5	0.935
3	16	10	5	1.010
4	0	8	5	0.546
5	6	6	5	0.936
6	13	6	5	1.067

Scale → q/q_∞ = 1 → Model 1.3101

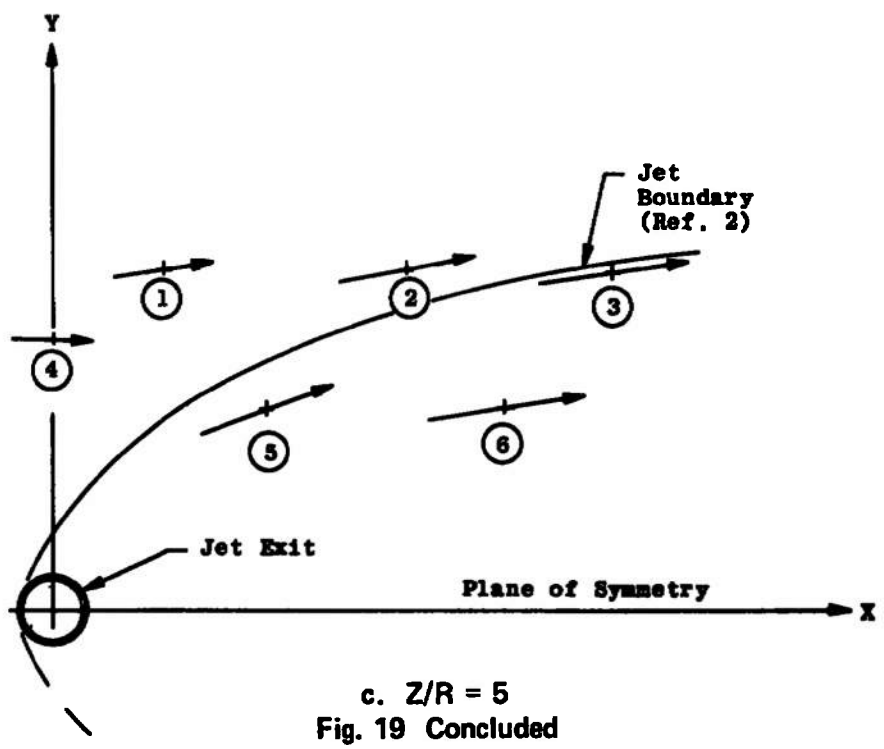

c. Z/R = 5

Fig. 19 Concluded

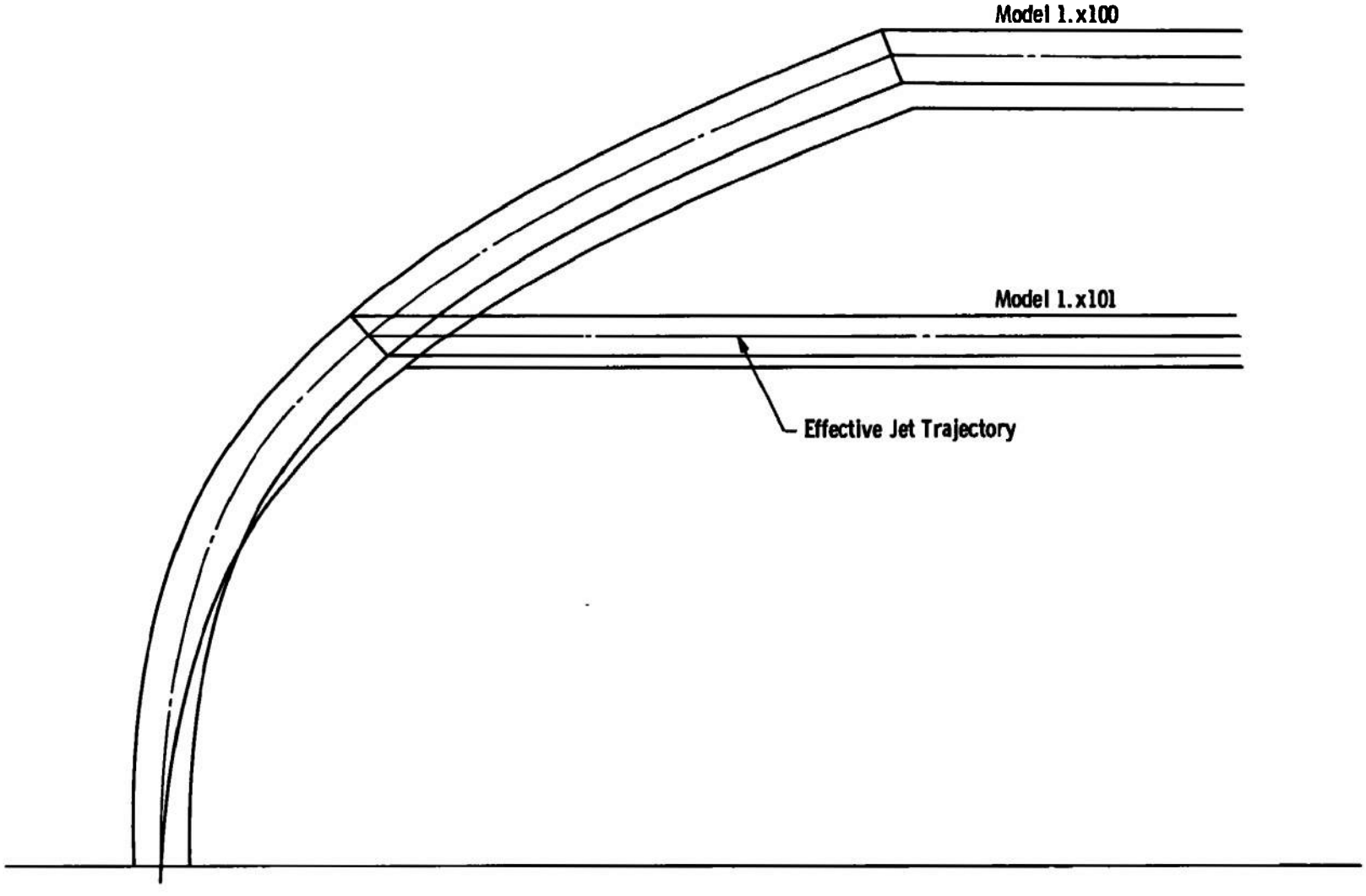

Fig. 20 Schematic of Vortices Trailing from Models 1.x100 and 1.x101

Point	X/R	Y/R	Z/R	q/q_∞	
				Mosher	1.4100
1	6	1	24	0.95	0.634
2	6	6	24	0.93	1.173
3	6	10	24	1.02	1.214
4	6	2	10	3.51	1.863
5	6	10	12	1.30	1.740
6	6	6	5	1.21	1.481
7	6	10	5	1.20	1.416

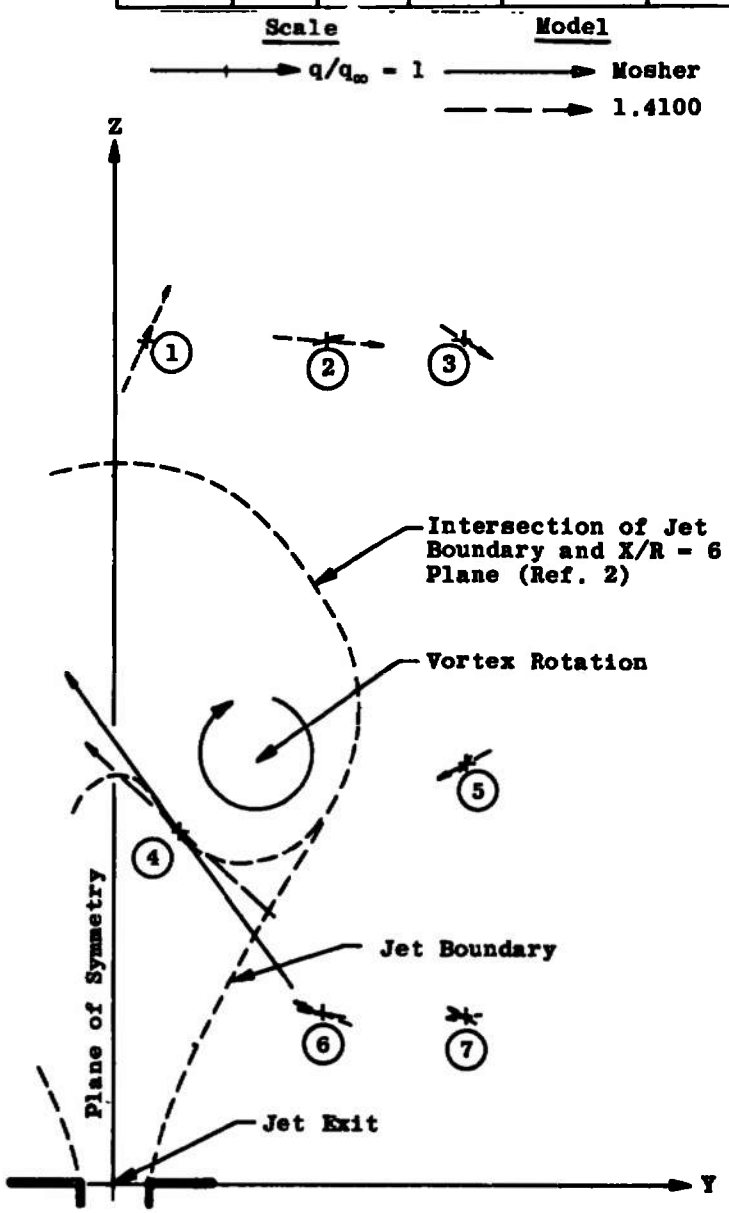

a. X/R = 6

Fig. 21 Comparison of Experimental Data and Model 1.4100 Analytical q-Vector Projections

Point	X/R	Y/R	Z/R	q/q_∞	
				Mosher	1.4100
1	6	10	24	1.02	1.214
2	6	10	12	1.30	1.740
3	3	10	5	1.25	1.506
4	10	10	5	1.14	1.268
5	16	10	5	1.07	1.121

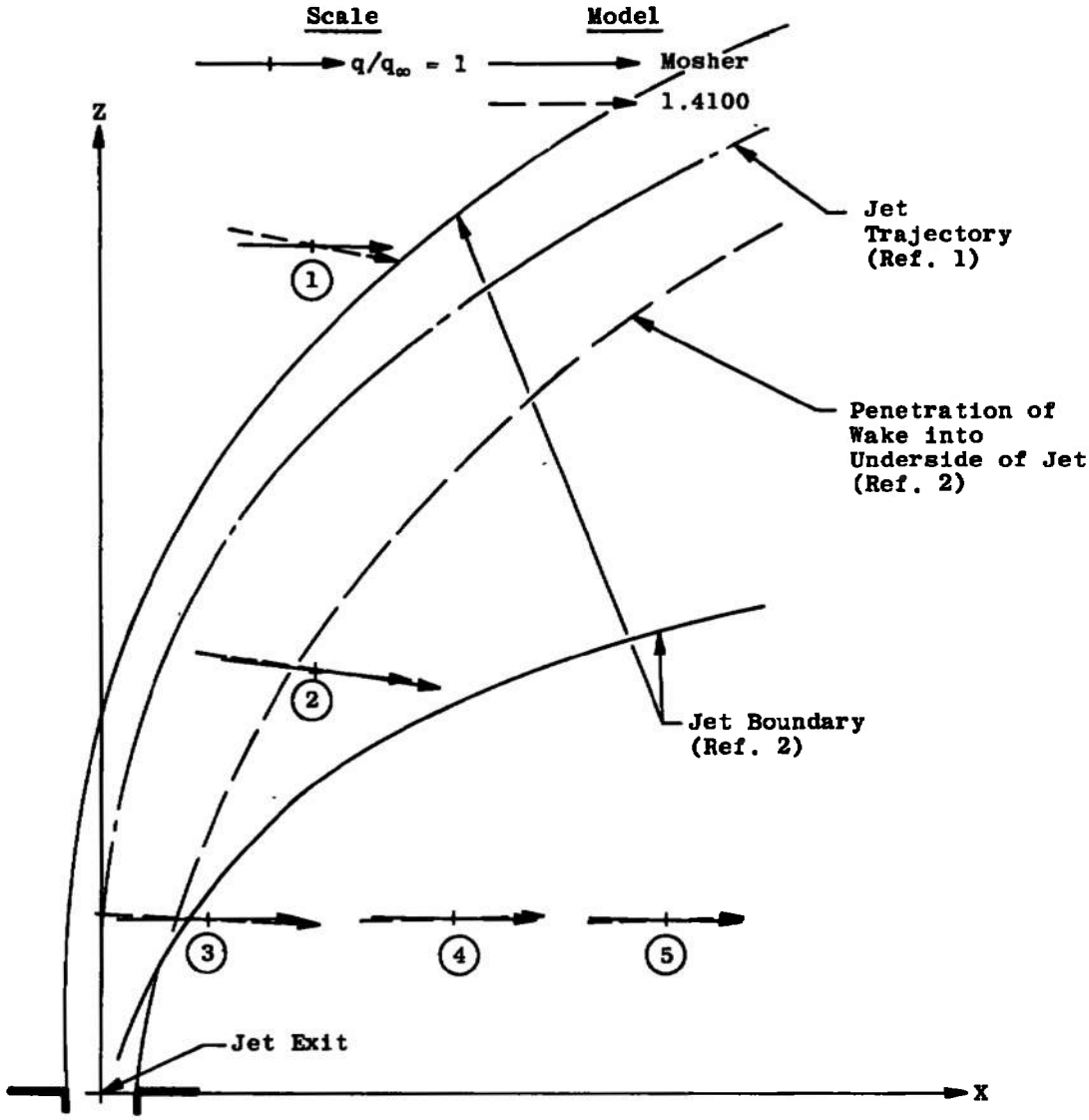

b. Y/R = 10

Fig. 21 Continued

Point	X/R	Y/R	Z/R	q/q_∞	
				Mosher	1.4100
1	3	10	5	1.25	1.506
2	10	10	5	1.14	1.268
3	16	10	5	1.07	1.121
4	0	8	5	1.33	1.667
5	6	6	5	1.21	1.481
6	13	6	5	1.04	1.113

Scale — $q/q_\infty = 1$

Model — Mosher; 1.4100

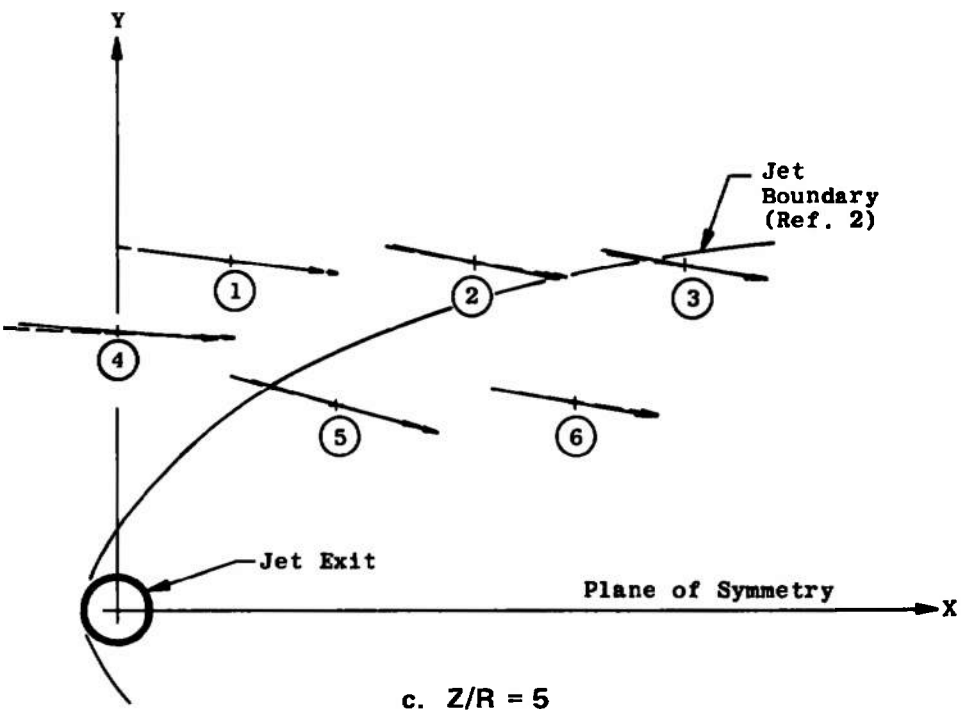

c. Z/R = 5

Fig. 21 Concluded

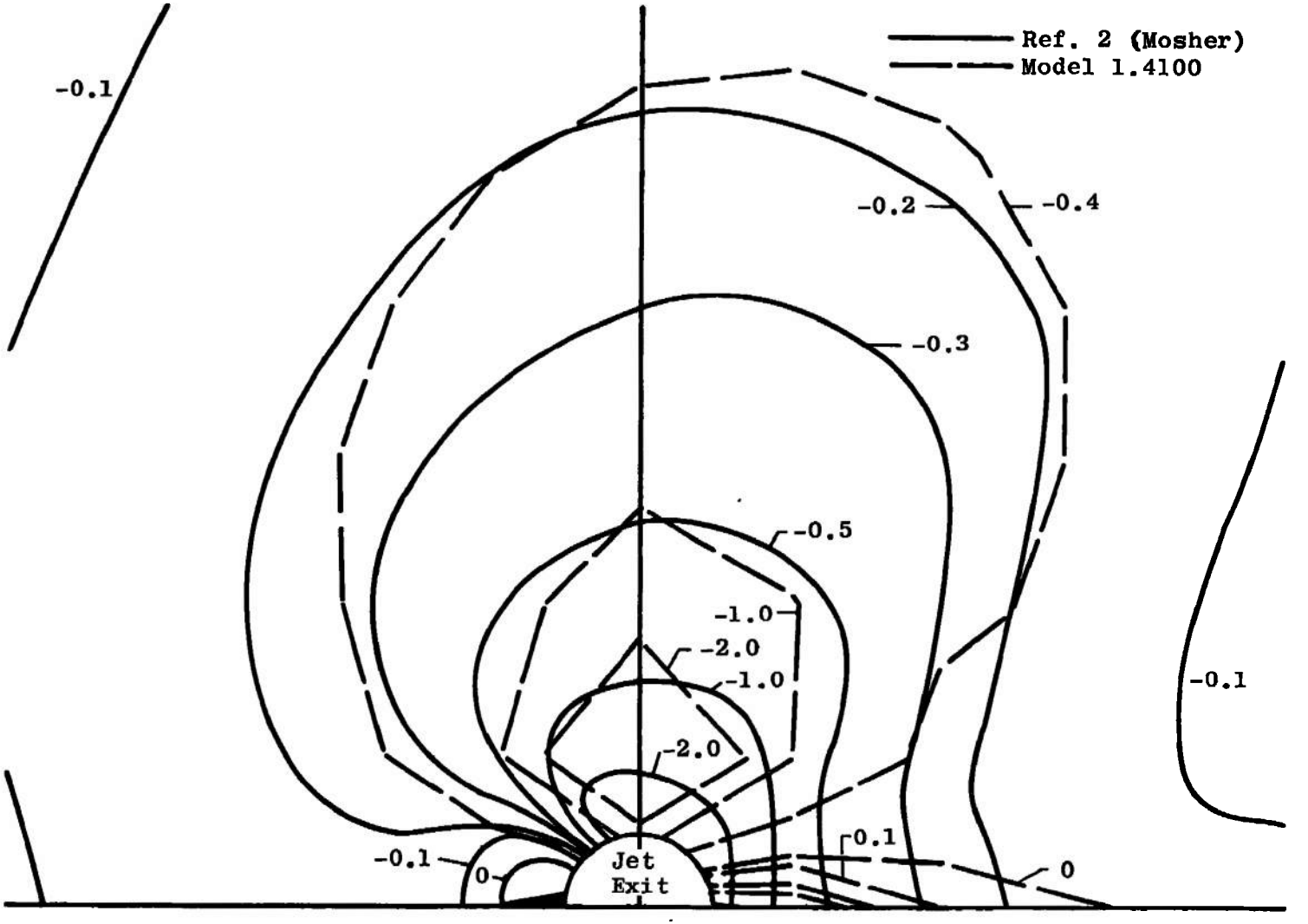

Fig. 22 Comparison of Computed Pressure Coefficient Contours for Model 1.4100 with Ref. 2 Experimental Data

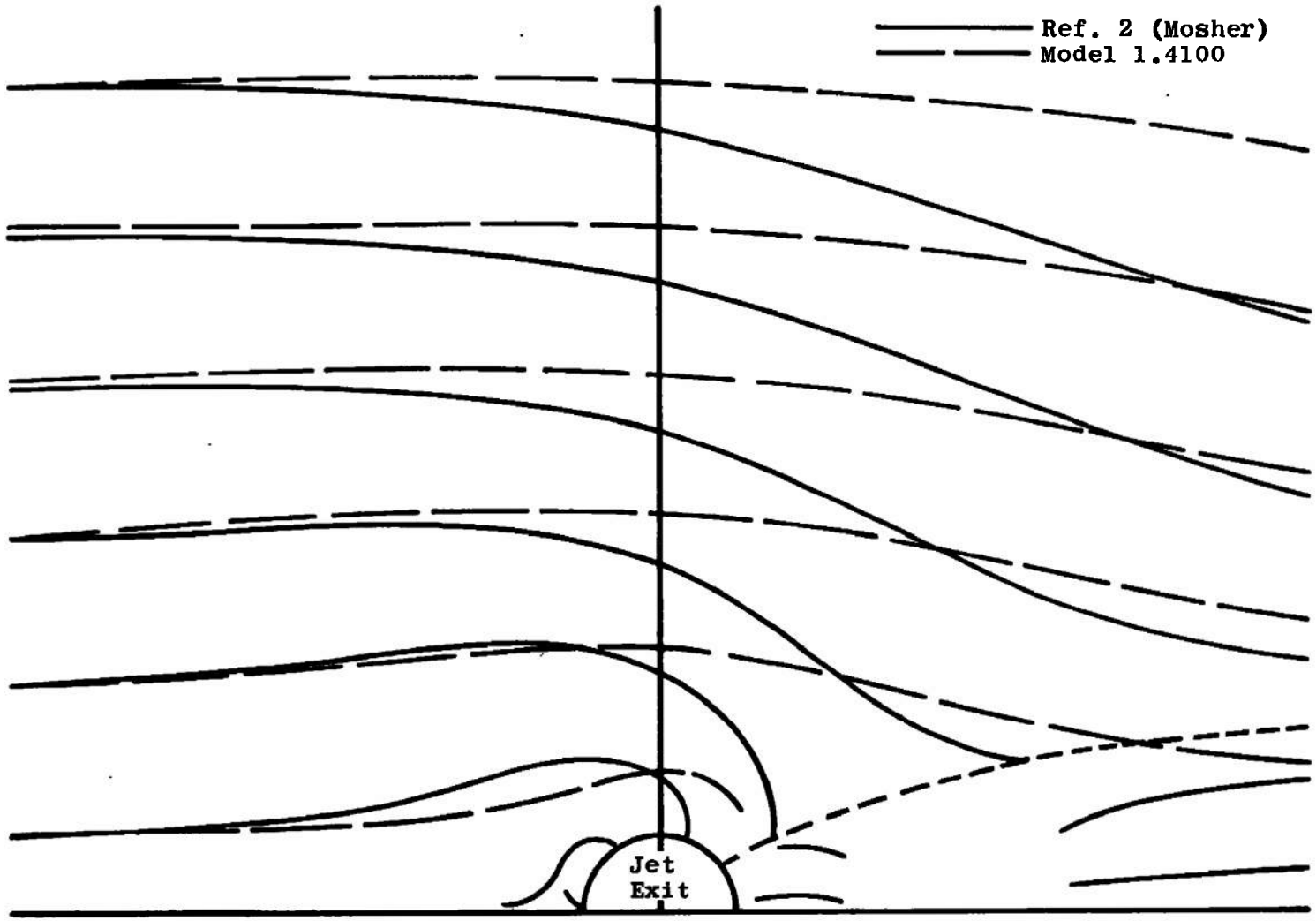

Fig. 23 Comparison of Computed Streamlines for Model 1.4100 with Ref. 2 Experimental Data

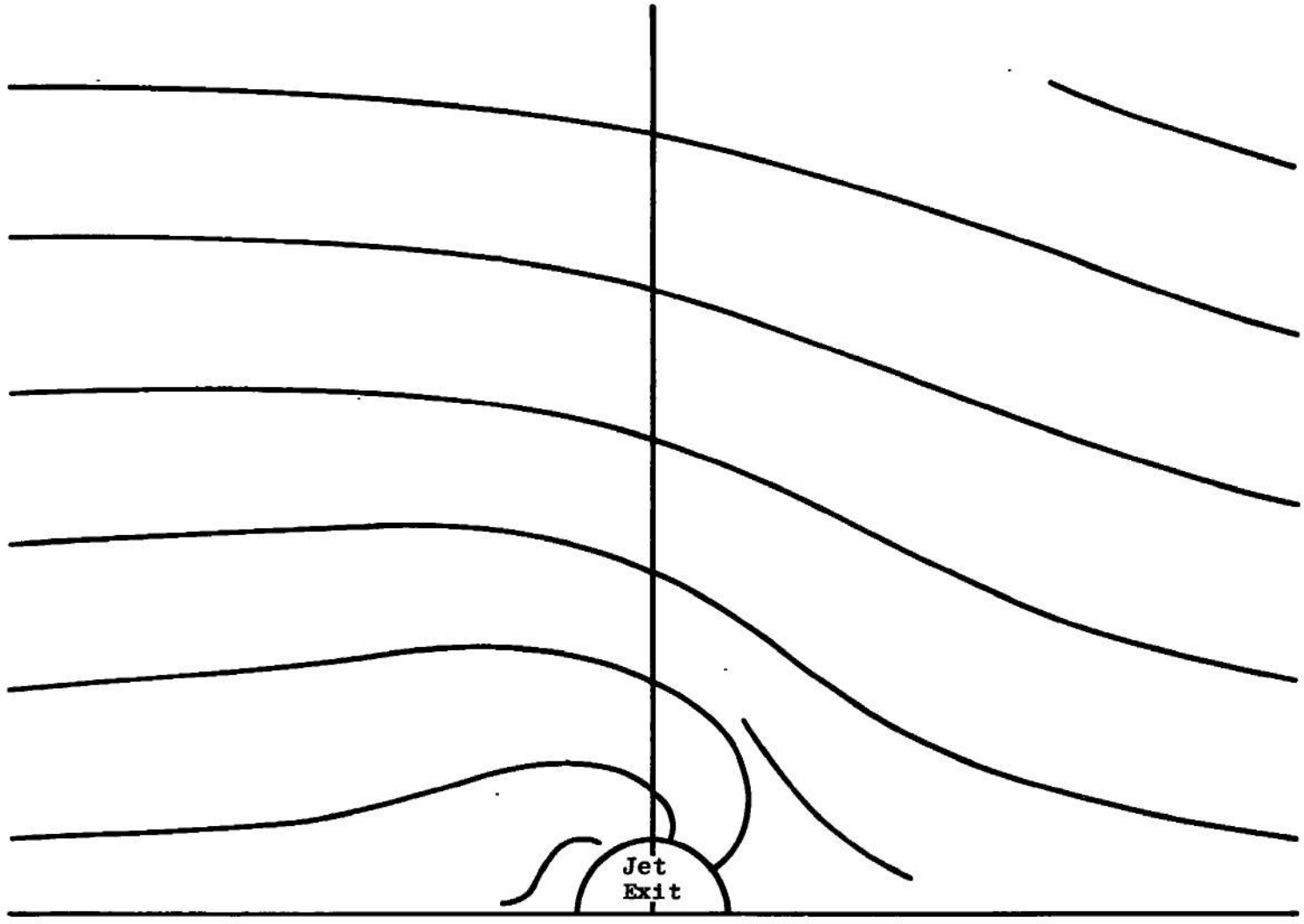

Fig. 24 Proposed Real Streamlines Immediately Above the Surface Disturbances

TABLE I
KEY TO MODEL IDENTIFICATION NUMBERS

Model Number	First Digit, V_j/V_∞	Second Digit, Entrainment Rate	Third Digit, Effective Jet Expansion Rate	Fourth Digit, Vortex Sheet Width	Fifth Digit, Vortex Ring Spacing
1.0000	8.0	0.0	(1)	(1)	(2)
1.1000	↓	0.02	(1)	↓	↓
1.2000		0.04	(1)		
1.2100		0.04	(3)		
1.3000		0.10	(1)		
1.3100		0.10	(3)		
1.3101		0.10	↓		(4)
1.4100		0.64		↓	(2)
1.4110		0.64		(5)	(2)
1.5100	↓	1.30	↓	(1)	(2)

LEGEND

(1) Same as contour used in propeller configuration (Ref. 3)

(2) 0.9 jet diam from jet exit to first ring, distance increased by 0.24 jet diam for each successive ring

(3) Original contour elongated by $2.1 \times (V_j V_\infty)$

(4) 0.45 jet diam from jet exit to first ring, distance increased by 0.12 jet diam for each successive ring

(5) Original contour widened by 200 percent

UNCLASSIFIED
Security Classification

DOCUMENT CONTROL DATA - R & D

(Security classification of title, body of abstract and indexing annotation must be entered when the overall report is classified)

1 ORIGINATING ACTIVITY (Corporate author)
Arnold Engineering Development Center
Arnold Air Force Station, Tennessee 37389

2a. REPORT SECURITY CLASSIFICATION
UNCLASSIFIED

2b GROUP
N/A

3 REPORT TITLE
APPLICATION OF THE VORTEX-LATTICE METHOD TO REPRESENT A JET EXHAUSTING FROM A FLAT PLATE INTO A CROSSFLOWING STREAM

4 DESCRIPTIVE NOTES (Type of report and inclusive dates)
Final Report -- July 1, 1970, to June 30, 1971

5 AUTHOR(S) (First name, middle initial, last name)
F. L. Heltsley and R. L. Parker, Jr., ARO, Inc.

6 REPORT DATE	7a. TOTAL NO OF PAGES	7b NO OF REFS
June 1973	72	8

8a. CONTRACT OR GRANT NO	9a. ORIGINATOR'S REPORT NUMBER(S)
b. PROJECT NO 69BT	AEDC-TR-73-57
c Program Element 64207F	9b. OTHER REPORT NO(S) (Any other numbers that may be assigned this report)
d.	ARO-OMD-TR-72-173

10. DISTRIBUTION STATEMENT
Approved for public release; distribution unlimited.

11 SUPPLEMENTARY NOTES	12 SPONSORING MILITARY ACTIVITY
Available in DDC.	Air Force Flight Dynamics Laboratory (AFFDL/FDDM), Air Force Systems Command, Wright-Patterson AFB, OH 45433

13 ABSTRACT

A study was conducted to develop a mathematical model of a jet exhausting from a flat plate into a crossflowing stream. The modeling was accomplished using the vortex-lattice method. Analytical streamlines and pressure distributions on the flat-plate surface as well as vector data in the field above the plate are compared with available experimental data. Recommendations are made for further improvement of vortex-lattice jet-modeling techniques.

DD FORM 1 NOV 65 1473

UNCLASSIFIED
Security Classification

14. KEY WORDS	LINK A		LINK B		LINK C	
	ROLE	WT	ROLE	WT	ROLE	WT
digital simulation						
flow distribution						
flat plate models						
V/STOL						
vertical takeoff aircraft						
jets						
fluid flow						
downwash						

AFSC
Arnold AFS Tenn.